



The limiting factors and regulatory processes that control the environmental responses of C₃, C₃–C₄ intermediate, and C₄ photosynthesis

Jennifer E. Johnson¹ · Christopher B. Field^{1,2} · Joseph A. Berry¹

Received: 7 August 2020 / Accepted: 7 October 2021 / Published online: 29 October 2021
© The Author(s) 2021

Abstract

Here, we describe a model of C₃, C₃–C₄ intermediate, and C₄ photosynthesis that is designed to facilitate quantitative analysis of physiological measurements. The model relates the factors limiting electron transport and carbon metabolism, the regulatory processes that coordinate these metabolic domains, and the responses to light, carbon dioxide, and temperature. It has three unique features. First, mechanistic expressions describe how the cytochrome b₆f complex controls electron transport in mesophyll and bundle sheath chloroplasts. Second, the coupling between the mesophyll and bundle sheath expressions represents how feedback regulation of Cyt b₆f coordinates electron transport and carbon metabolism. Third, the temperature sensitivity of Cyt b₆f is differentiated from that of the coupling between NADPH, Fd, and ATP production. Using this model, we present simulations demonstrating that the light dependence of the carbon dioxide compensation point in C₃–C₄ leaves can be explained by co-occurrence of light saturation in the mesophyll and light limitation in the bundle sheath. We also present inversions demonstrating that population-level variation in the carbon dioxide compensation point in a Type I C₃–C₄ plant, *Flaveria chloroefolia*, can be explained by variable allocation of photosynthetic capacity to the bundle sheath. These results suggest that Type I C₃–C₄ intermediate plants adjust pigment and protein distributions to optimize the glycine shuttle under different light and temperature regimes, and that the malate and aspartate shuttles may have originally functioned to smooth out the energy supply and demand associated with the glycine shuttle. This model has a wide range of potential applications to physiological, ecological, and evolutionary questions.

Keywords Cytochrome b₆f · Rubisco · Glycine decarboxylase · CO₂ compensation point · Temperature

Introduction

At present, the major patterns in the ecology and evolution of C₃ and C₄ plants are attributed to the physiological differences between the C₃ and C₄ photosynthetic pathways. The foundation for this theory is the observation that the two pathways translate into distinct physiological advantages and disadvantages under different environmental conditions (Berry 1975; Ehleringer and Björkman 1977). C₃

photosynthesis provides advantages over C₄ photosynthesis under low light intensities, high carbon dioxide levels, and cool temperatures, while C₄ photosynthesis provides advantages over C₃ photosynthesis under high light intensities, low carbon dioxide levels, and warm temperatures (Berry and Björkman 1980; Berry and Downton 1982; Pearcy and Ehleringer 1984). These physiological trade-offs are thought to be the basis of the evolutionary rise of C₄ plants in ancient environments characterized by lower atmospheric carbon dioxide (Monson 1989a; Ehleringer and Monson 1993; Ehleringer et al. 1997; Osborne and Beerling 2006; Tipple and Pagani 2007; Osborne and Sack 2012). They are also thought to be the basis of the ecological dominance of C₄ plants in modern environments characterized by high light intensities, warm temperatures, and a moderate amount of warm season precipitation (Ehleringer 1978; Ehleringer and Monson 1993; Collatz et al. 1998; Still et al. 2003). However, it is not yet clear how to reconcile these ideas with the

Communicated by Paul Stoy.

✉ Jennifer E. Johnson
jjohnson@carnegiescience.edu

¹ Department of Global Ecology, Carnegie Institution for Science, 260 Panama Street, Stanford, CA 94305, USA

² Stanford Woods Institute for the Environment, Stanford University, 473 Via Ortega, Stanford, CA 94305, USA

physiology, ecology, and evolution of plants that use C₃–C₄ intermediate photosynthesis.

On the one hand, a number of lines of evidence suggest that C₃–C₄ intermediate photosynthesis represents an intermediate stage in evolutionary transitions between C₃ and C₄ photosynthesis (Kennedy and Laetsch 1974; Christin et al. 2011; Sage et al. 2014; Stata et al. 2019; Lyu et al. 2021). On the other hand, no ecological conditions have yet been identified under which C₃–C₄ intermediate photosynthesis provides C₃–C₄ plants with unique physiological advantages over C₃ as well as C₄ plants (Monson et al. 1984, 1986; Peisker 1986; von Caemmerer 1989; Monson 1989a, 2003; Ehleringer and Monson 1993; Ehleringer et al. 1997; Sage et al. 2012, 2018; Heckmann et al. 2013; Christin and Osborne 2014; Lundgren and Christin 2017). The simplest way to reconcile these observations would be to posit that there are some ecological conditions under which C₃–C₄ intermediate photosynthesis can represent an evolutionarily stable strategy (Maynard Smith and Price 1973), and the exact nature of these conditions simply remains to be elucidated. But this may or may not be the right interpretation. At the heart of this puzzle is the question: what are the relative advantages and disadvantages of C₃, C₃–C₄ intermediate, and C₄ photosynthesis?

We submit that to answer this question, it is necessary to directly confront the current conceptual models of the C₃, C₃–C₄ intermediate, and C₄ pathways with experimental measurements. Towards this end, the objective of this paper is to describe a general model of C₃, C₃–C₄ intermediate, and C₄ photosynthesis that is designed to facilitate quantitative analysis of physiological measurements. This model uses the approach introduced by Johnson and Berry (2021) to describe how the overall photosynthetic responses to light, carbon dioxide, and temperature emerge from the factors limiting electron transport and carbon metabolism and the regulatory processes that coordinate these metabolic domains. In the remainder of the Introduction, we review current understanding of C₃, C₄, and C₃–C₄ intermediate photosynthesis and outline the philosophy that has guided the development of this modeling framework. In Model Development we then introduce the key features of this framework and in Model Applications we present example applications to the interpretation of physiological measurements.

The C₃ photosynthetic pathway

The current understanding of C₃ photosynthesis began to be assembled more than a century ago. In the early 1900s, it was established that C₃ photosynthesis involves the coordinated operation of two metabolic domains with different sensitivities to light, carbon dioxide, and temperature (Blackman 1905). During the 1910–1920s, it was inferred

that at low light intensities the overall process is controlled by ‘a photochemical reaction’ with low temperature sensitivity, whereas at high light intensities the control shifts to a ‘purely chemical reaction’ with much higher temperature sensitivity (Emerson 1929). During the 1930–1960s, the nature of these processes was pursued. It was shown that the metabolic domain in control at low light is the electron transport system, and that it operates in two major modes. One is a linear electron flow that involves two photochemical reactions, splits water, and leads to the net production of oxygen, Fd, NADPH, and ATP (Duygens et al. 1961). The other is a cyclic electron flow that only involves one photochemical reaction and leads to the net production of ATP (Tagawa et al. 1963). The pigment-protein complexes mediating the photochemical reactions are now known as Photosystem II (PS II; EC 1.10.3.9) and Photosystem I (PS I; EC 1.97.1.12). In parallel, it was shown that the metabolic domain in control at high light is carbon metabolism, and that it also operates in two major modes: a photosynthetic carbon reduction cycle which fixes CO₂ (Calvin and Benson 1948) and a photosynthetic carbon oxidation cycle which fixes O₂ (Tregunna et al. 1966). During the late 1960s and early 1970s, the sites of the primary rate-limitations were identified within both metabolic domains. The primary rate-limiting factor within the electron transport system was found to be the Cytochrome b₆f complex (Cyt b₆f; EC 7.1.1.6), which participates in linear as well as cyclic electron flow (Stiehl and Witt 1969). The primary rate-limiting factor within carbon metabolism was found to be Ribulose-1,5-bisphosphate carboxylase/oxygenase (Rubisco; EC 4.1.1.39), which participates in the photosynthetic carbon reduction and oxidation cycles (Ogren and Bowes 1971; Bowes et al. 1971; Laing et al. 1974). During the 1980s and 1990s, advances were made in identifying the regulatory processes that mediate flux in between these limits. It was established that under saturating light there is downregulation of many of the membrane-bound enzymes in the electron transport system, including Cyt b₆f, whereas under limiting light there is downregulation of many of the stromal enzymes involved in carbon metabolism, including Rubisco (Heber et al. 1986; Weis et al. 1987; Harbinson et al. 1990). In combination, these insights underpin current conceptual understanding of how the C₃ photosynthetic pathway operates as an integrated system in dynamic environments.

The development of quantitative models of C₃ photosynthesis proceeded in parallel with the development of conceptual understanding. Initially, the light response of photosynthesis was described as having a domain where the photosynthetic rate increases linearly with light, and a sharp transition to another domain where the CO₂ supply becomes limiting (Blackman 1905). A rectangular hyperbolic function was then introduced to provide a smoother transition from the light-limited and CO₂-limited parts of

the response (Rabinowitch 1951). This was eventually supplanted by a more flexible non-rectangular hyperbola, which included an additional parameter to describe the degree of curvature of the light response (Thornley 1976). The non-rectangular hyperbolic description of the light response was then linked to a mechanistic expression for Rubisco based on competitive inhibition between CO₂ and O₂ (Farquhar et al. 1980a). This formulation is effective at approximating the environmental responses of gas-exchange, but incorrectly predicts that the activity of the electron transport system limits the activity of carbon metabolism under saturating light and saturating CO₂. To address this issue, another model was developed that links a linear, Blackman-type light response to the mechanistic expression for Rubisco (Collatz et al. 1991). This framework correctly predicts that the activity of carbon metabolism limits the activity of the electron transport system under saturating light and saturating CO₂. Since it is effective at describing the states of regulation under different environmental conditions, it was also extended to simulate chlorophyll fluorescence (van der Tol et al. 2014). While this model performs well when it can be calibrated directly, it is still empirical and the predictive skill degrades outside the calibration domain. To address this issue, we have recently developed a new model that links a Cyt b₆f-based description of the light response to the Rubisco-based description of the CO₂ response (Johnson and Berry 2021). By describing the light response mechanistically rather than empirically, the model can be used to infer the state of regulation under different light intensities and CO₂ levels. This permits more accurate and efficient simulation of gas-exchange, chlorophyll fluorescence, and other optical probes of electron transport. It also provides a new basis for analyzing how the temperature sensitivities of the electron transport system contribute to the overall temperature response of photosynthesis. The latter is a key priority both for understanding the C₃ pathway itself, and for understanding the relative advantages and disadvantages of the C₃ relative to the C₄ pathway.

The C₄ photosynthetic pathway

Insights into the differences between C₃ and C₄ photosynthesis began to emerge during the 1960s. During this period, it was established that the C₃ pathway takes place entirely in leaf mesophyll cells, but the C₄ pathway involves both the mesophyll and bundle sheath. It was found that in C₄ photosynthesis, CO₂ from the mesophyll is initially fixed into oxaloacetate by PEP carboxylase (PEPC; EC 4.1.1.31) and oxaloacetate is converted to malate and/or aspartate (Kortschak et al. 1965; Slack and Hatch 1967). The organic acids were then found to be shuttled into the bundle sheath, where Rubisco is situated (Björkman and Gauhl 1969). During the 1970s, it was established that the

NADP-malic enzyme (NADP-ME; EC 1.1.1.40), NAD-malic enzyme (NAD-ME; EC 1.1.1.39), and/or PEP carboxykinase (PEPCK; EC 4.1.1.49) decarboxylates the organic acids in the bundle sheath, releasing CO₂ in the vicinity of Rubisco (Hatch et al. 1975). In combination, these observations indicated that the primary rate-limiting factor in mesophyll carbon metabolism is PEP carboxylase, while that in bundle sheath carbon metabolism is Rubisco. During the 1980s, the relationship between cell type-specific patterns of carbon metabolism and electron transport was pursued. It was found that the distinct energetic requirements of mesophyll and bundle sheath carbon metabolism are supported by modifications in linear and cyclic flow within each cell type, and that these vary depending on the decarboxylation pathway (Chapman et al. 1980; Hatch 1987). This suggested that the efficient operation of the C₄ pathway requires cell type-specific balancing of the absorption cross-sections of PS I and PS II in relation to the primary kinetic bottleneck at Cyt b₆f. During the 1990s, there were initial advances in understanding the regulatory processes that coordinate flux between the limits set by Cyt b₆f, PEPC, and Rubisco. In addition to the forms of regulation evident in the C₃ cycle, it was established that under limiting light there is down-regulation of PEPC that is coordinated with that of other enzymes in the C₄ cycle (Furbank and Taylor 1995; Chollet et al. 1996; Leegood and Walker 1999). This reinforced the earlier idea that regulation of rate-limiting steps is the general way of maintaining coordination between electron transport and carbon metabolism. However, the conceptual understanding of how the C₄ photosynthetic pathway operates as an integrated system in dynamic environments has remained relatively less clear and less comprehensive than analogous understanding of the C₃ photosynthetic pathway. Due to the complexity of the C₄ system, there is a need and an opportunity for modeling to contribute here.

The development of quantitative models of C₄ photosynthesis has been closely linked to the development of quantitative models of C₃ photosynthesis. In the late 1970s, a conceptual model was formulated that represented PEPC activity in the mesophyll as the rate-limiting step in the initial fixation of CO₂, transport of organic acids and decarboxylation in the bundle sheath (Berry and Farquhar 1978). This model demonstrated that when the C₄-cycle pumps CO₂ into the bundle sheath faster than CO₂ leaks out of the bundle sheath, the resulting increase in the bundle sheath CO₂ relative to O₂ competitively inhibits O₂ fixation, allowing Rubisco to operate close to its maximal rate of CO₂ fixation. Similar to the C₃ models formulated around this time, this formulation is effective at approximating the environmental responses of gas-exchange, but incorrectly predicts that the activity of the electron transport system limits the activity of carbon metabolism under saturating light and saturating CO₂. During the 1990s, another model

was developed that addressed this issue by linking a linear, Blackman-type light response to mechanistic expressions for PEPC and Rubisco (Collatz et al. 1992). However, this model also intentionally simplified the kinetic descriptions of PEPC and Rubisco to facilitate applications to larger-scale environmental simulations (Sellers et al. 1996a,b). It was later extended to simulate chlorophyll fluorescence (van der Tol et al. 2014). In a parallel strand of C₄ model development, the earlier non-rectangular hyperbolic expression for the light response was brought back in and was again linked to the complete kinetic expressions for PEPC and Rubisco (von Caemmerer and Furbank 1999; von Caemmerer 2000, 2021). In both of these strands of C₄ model development, the potential linear electron transport of the leaf has been modeled as a whole and then partially allocated to the C₃ and C₄ cycles. This approach was designed to provide a simple way to accommodate the variable contributions of the different C₄ decarboxylases and 3-phosphoglyceric acid export to the energy budget. A number of refinements of the stoichiometries associated with these processes have been proposed over the years (e.g., Furbank et al. 1990; Yin and Struik 2012, 2018, 2021; Bellasio 2017). However, the fundamental issue remains that all of these C₄ models are missing a fully mechanistic description of the light response, and this limits their ability to clearly explain the coordination between electron transport and carbon metabolism. This is a key priority for model development, and one that we will tackle here by progressively building up the components of the full C₄ pathway from their foundation in the C₃–C₄ intermediate pathways.

The C₃–C₄ intermediate photosynthetic pathways

When C₃–C₄ intermediate photosynthesis was originally discovered in the 1970s, it was clear that C₃–C₄ intermediate plants exhibited a sensitivity to O₂ that was intermediate between the sensitivities of C₃ and C₄ plants, but it was not clear what mechanism(s) were responsible for this (Kennedy and Laetsch 1974). Two conceptual models were considered: one in which the intermediate sensitivity to O₂ was due to low levels of C₄-cycle activity, and one in which it was due to refixation of CO₂ released from the photosynthetic carbon oxidation cycle (Monson et al. 1984). Before a mechanism was identified for the refixation of CO₂ released from the photosynthetic carbon oxidation cycle, a quantitative model of C₃–C₄ intermediate photosynthesis was developed based on the assumption that the physiological characteristics of C₃–C₄ intermediate plants were generated solely by low levels of C₄-cycle activity (i.e., via malate and/or aspartate shuttling; Peisker 1984, 1986; Peisker and Bauwe 1984). Following the discovery that the P-protein of the glycine decarboxylase (GDC; EC 1.4.4.2) complex was localized to the bundle sheath in C₃–C₄ intermediate plants, it became

clear that the physiological characteristics of some C₃–C₄ intermediate plants might be generated solely by recycling of CO₂ released from the photosynthetic carbon oxidation cycle within the bundle sheath (Hylton et al. 1988; i.e., via glycine shuttling; Rawsthorne et al. 1988a, b). Based on this conceptual model, von Caemmerer (1989, 1992) developed a new quantitative model to represent the glycine shuttle. Later, von Caemmerer (2000) synthesized the expressions developed by Peisker and Bauwe (1984), Peisker (1986), von Caemmerer (1989), and von Caemmerer (1992) into equations that could represent Type I, Type II, or C₄-like C₃–C₄ intermediate photosynthesis (Table 1). In the equation set described by von Caemmerer (2000), the basis of the glycine shuttle is the localization of some of the Rubisco activity and some or all of the GDC activity in the bundle sheath rather than in the mesophyll. Under environmental conditions that exacerbate Rubisco oxygenase activity in the mesophyll, this configuration leads to: (i) net production of glycine in the mesophyll; (ii) net diffusion of glycine into the bundle sheath; (iii) decarboxylation of that glycine within the bundle sheath, (iv) an increase in the bundle sheath CO₂/O₂ ratio, and (v) a corresponding increase in the efficiency of CO₂ fixation by the bundle sheath Rubisco. Under environmental conditions that exacerbate Rubisco oxygenase activity in the bundle sheath, (i)–(v) are reversed. As a result of this environmental sensitivity, there is not a fixed energetic cost or benefit associated with the glycine shuttle. Instead, the glycine shuttle tends to confer a net energetic benefit over the C₃ pathway under conditions that promote Rubisco oxygenase activity in the mesophyll, and a net energetic cost under conditions that suppress such activity.

At present, it is unclear whether this model is correct. Forward simulations based on these equations have generated predictions that Type I C₃–C₄ plants should exhibit higher rates of net CO₂ assimilation than C₃ plants under typical midday conditions (i.e., saturating light, moderate leaf temperatures, and modern atmospheric CO₂ and O₂ levels; von Caemmerer 1989, 2000; Schuster and Monson 1990; Monson and Rawsthorne 2000; Heckmann et al. 2013; Mallmann et al. 2014; Way et al. 2014; Bellasio and Farquhar 2019). All else being equal, there is a clear theoretical basis for expecting that such relative advantages in the net CO₂ assimilation rates should translate into corresponding advantages in the photosynthetic resource-use efficiencies (Field 1983; Field et al. 1983; Field and Mooney 1986; Monson 1989b; Schuster and Monson 1990; Monson and Rawsthorne 2000; Christin and Osborne 2014; Way et al. 2014; Lundgren 2020; Sundermann et al. 2021). However, Type I C₃–C₄ plants have not consistently exhibited higher photosynthetic rates, light-use efficiencies, water-use efficiencies, or nitrogen-use efficiencies than C₃ plants when measurements have been made under these conditions (Brown and Brown

Table 1 Functional distinctions between C₃, C₃–C₄, and C₄ photosynthesis

Pathway	Enzyme localization					Bundle sheath CO ₂ source		
	PS I & II	Cyt b ₆ f	Rubisco	GDC	PEPC	Glycine shuttle	Malate shuttle	Aspartate shuttle
C ₃	M	M	M	M	–	–	–	–
Proto-Kranz C ₃ –C ₄	M, BS	M, BS	M, BS	M, BS	–	Low activity	–	–
Type I C ₃ –C ₄	M, BS	M, BS	M, BS	BS	–	High activity	–	–
Type II C ₃ –C ₄	M, BS	M, BS	M, BS	BS	M	High activity	Low activity	Low activity
C ₄ -like C ₃ –C ₄	M, BS	M, BS	M, BS	BS	M	Low activity	Variable activity	Variable activity
NADP-ME C ₄	M, BS	M, BS	BS	BS	M	–	High activity	Variable activity
NAD-ME C ₄	M, BS	M, BS	BS	BS	M	–	Variable activity	High activity
PEPCK C ₄	M, BS	M, BS	BS	BS	M	–	Variable activity	Variable activity

Traditionally, the categorization of C₃–C₄ and C₄ plants into discrete ‘types’ has been used to emphasize general patterns of functional similarities and differences. However, it is important to recognize that many biochemical and anatomical attributes of these plants exhibit continuous variation. PS I Photosystem I, PS II Photosystem II, Cyt b₆f Cytochrome b₆f complex, Rubisco Ribulose-15-bisphosphate carboxylase-oxygenase, GDC Glycine decarboxylase complex, PEPC PEP carboxylase, NADP-ME NADP-malic enzyme, NAD-ME NAD-malic enzyme, PEPCK PEP carboxykinase, M mesophyll, BS bundle sheath

1975; Brown and Simmons 1979; Bolton and Brown 1980; Ehleringer and Pearcy 1983; Henning and Brown 1986; Monson et al. 1986; Fladung and Hesselbach 1989; Monson 1989b; Krall et al. 1991; Ku et al. 1991; Monson and Rawsthorne 2000; Huxman and Monson 2003; Voznesenskaya et al. 2007; Vogan et al. 2007; Pinto et al. 2011, 2014; Vogan and Sage 2011, 2012; Khoshravesh et al. 2016; Lundgren et al. 2016). From a quantitative perspective, there are two explanations for the discrepancy between the observations and predictions: either (i) there is a fundamental problem with the structure of the model of C₃–C₄ photosynthesis, or (ii) the structure of the model is correct, but there is a fundamental problem with the parameterizations used for the simulations. For example, it has been suggested that the strong light dependence of the CO₂ compensation point may indicate that C₃–C₄ photosynthesis does not work exactly as described above (von Caemmerer 2000). The most straightforward way to differentiate between this type of structural error versus a parameterization error is to fit the C₃–C₄ model to physiological measurements, objectively evaluate the quality of the fit between the model and the measurements, and compare the measurement-derived parameter set to the parameter set specified for the simulations. With this approach, the quality-of-fit statistics can be used to identify problems with model structure (i.e., testing the first hypothesis), and the inverse parameter estimates can be used to identify problems with model parameterization (i.e., testing the second hypothesis). To enable this mode of analysis, we will rely on the approach introduced by Johnson and Berry (2021) and described below.

A general framework for modeling C₃, C₃–C₄, and C₄ photosynthesis

Although inverse fitting has started to become established as an approach for interpreting physiological measurements of C₃ and C₄ plants, it is still not widely used and has not yet been applied to C₃–C₄ plants (e.g., Yin et al. 2009, 2011; Bellasio et al. 2016; Zhou et al. 2019). The main reason for this is that none of the current C₃, C₃–C₄, and C₄ models are formulated in a way that is ideal for fitting to experimental data. On the one hand, in the type of models that are simple enough to be fit directly to data and that we have discussed here, a large fraction of the key parameters are empirical (e.g., the θ and J_{\max} parameters describing the curvature and asymptote of the light response, respectively). Since there is no way to independently evaluate the fitted values of the empirical parameters in these frameworks, it is difficult to differentiate between problems with model structure versus model parameterization. On the other hand, in more complex models where a larger fraction of the parameters are mechanistic, there are simply too many free variables to constrain with typical experimental observations (e.g., Laisk and Edwards 2000; Laisk et al. 2009; Zhu et al. 2013; Wang et al. 2014, 2017, 2021; Morales et al. 2018). Since there is no way to rigorously confront the hypotheses in these frameworks with data, it is also difficult to differentiate between problems with model structure versus model parameterization. To address these challenges and opportunities, we have developed a general model of C₃, C₃–C₄, and C₄ photosynthesis that is designed to facilitate inverse analysis of physiological measurements (Fig. 1).

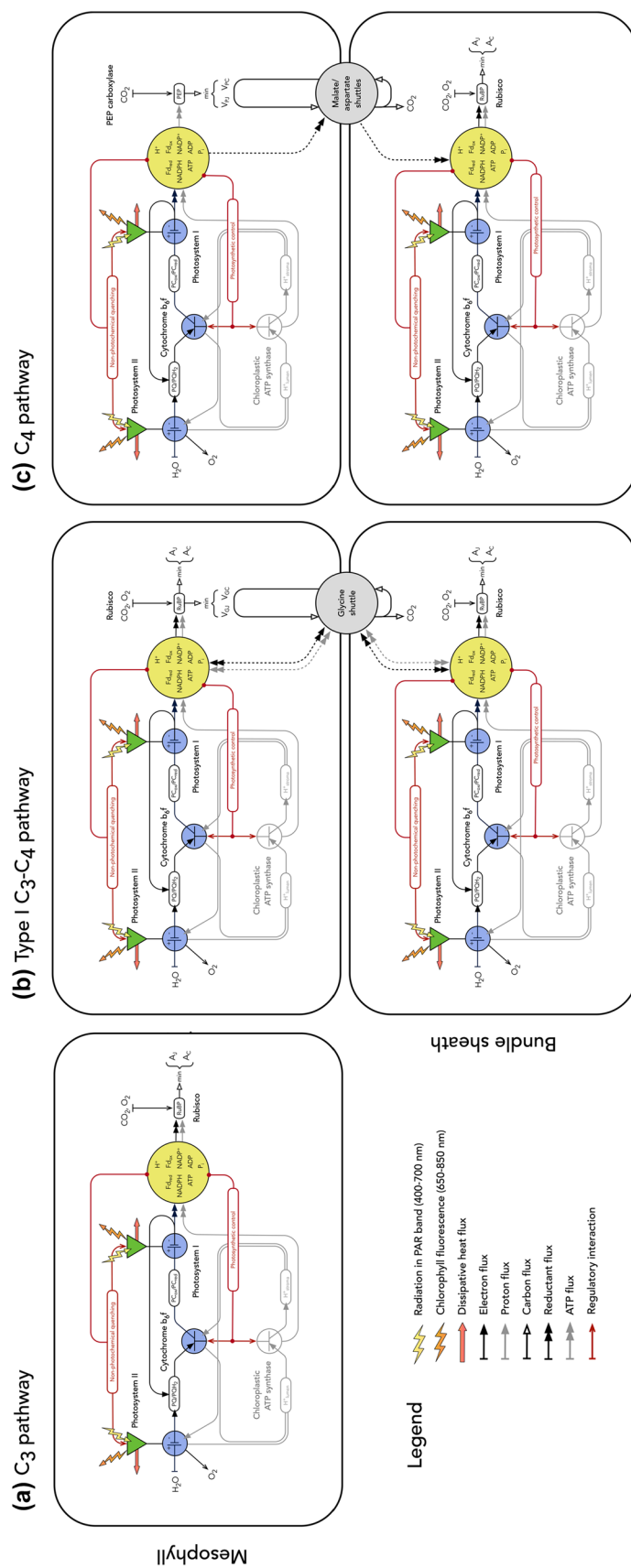


Fig. 1 Circuit diagrams for C₃, C₃-C₄ intermediate, and C₄ photosynthesis. **a** The C₃ case follows Johnson and Berry (2021). **b** The Type I C₃-C₄ intermediate case represents both the mesophyll and bundle sheath, and their coupling through the glycine shuttle. **c** The C₄ case represents the localization of all Rubisco activity to the bundle sheath, and the delivery of CO₂ from the mesophyll to bundle sheath through the malate and/or aspartate shuttles. Details are provided in text

The new model is organized around three design criteria. *First, this framework is designed to describe the overall photosynthetic process at the leaf-level when it has achieved a fully reversible steady-state with the measuring environment.* At this spatial and temporal scale, the dynamics of photosynthesis are much simpler than they are within particular sub-systems and/or during transient adjustments because they become keyed to the boundary conditions imposed by energy, mass, and charge balance. This makes this scale a tractable starting point for mathematical analysis. *Second, this framework is designed to link the photosynthetic process to the full suite of observable quantities that can be evaluated via leaf-level measurements.* Most current frameworks for modeling leaf-level photosynthesis are organized around trace gas concentration and/or isotope ratio measurements. Here, we have formulated a model that can also communicate with a diverse array of fluorescence- and absorbance-based measurements. *Third, this framework is designed to explain the environmental, biochemical, and anatomical factors that control the patterns of photosynthetic performance.* In formulating this model, we have avoided empirical descriptions that rely on statistical coefficients without precise physical meaning, as well as putatively mechanistic descriptions that are untestable. Instead, we have articulated hypotheses about the specific mechanisms that give rise to the observed patterns, and we have done so in a way that permits these hypotheses to be evaluated with independent measurements.

The new model brings together the description of C₃ electron transport from Johnson and Berry (2021) with the descriptions of C₃, C₃–C₄, and C₄ carbon metabolism from Berry and Farquhar (1978), Farquhar et al. (1980a), Farquhar and von Caemmerer (1981), von Caemmerer and Farquhar (1981), Peisker and Bauwe (1984), Peisker (1986), von Caemmerer (1989), Collatz et al. (1991), Collatz et al. (1992), von Caemmerer and Furbank (1999), von Caemmerer (2000), von Caemmerer et al. (2009), von Caemmerer (2013), van der Tol et al. (2014), von Caemmerer (2020, 2021). The resulting framework describes the steady-state responses of C₃, C₃–C₄, and C₄ photosynthesis to variation in light, carbon dioxide, and temperature. While the model can generate simulations over arbitrarily wide ranges of measurement light intensities, carbon dioxide levels, and leaf temperatures, it does not represent stress responses. As a result, the descriptions of regulatory interactions are only accurate within the ranges of conditions that leaves have acclimated to during growth. The equations that correspond to the schematic in Fig. 1 are presented in Appendices I–V in the Electronic Supplementary Material. To draw attention to the core aspects of model structure, we focus on the C₃, Type I C₃–C₄, and NADP-ME C₄ cases (Table 1), and we illustrate these cases using a simplified model

parameterization (Table 2). In the next section (Model Development), we discuss the series of three steps in model development, emphasizing the rationale for and theory underlying each step. In the subsequent section (Model Application), we then demonstrate how these developments come together in a way that enables the model to be applied for the quantitative interpretation of physiological measurements.

Model development

In this model, we use the mechanistic description of electron transport from Johnson and Berry (2021) to represent the potential electron transport capacities of the mesophyll chloroplasts and bundle sheath chloroplasts separately. This creates a foundation for analyzing the mechanisms of energy sharing between the mesophyll and bundle sheath. We begin by introducing the Cyt b₆f-based expression for electron transport and replicating it for the mesophyll and bundle sheath. Next, we discuss a hierarchical solution to the model that permits the mesophyll and bundle sheath to transition independently between limitation by electron transport and carbon metabolism. Finally, we turn to the formulation of the temperature response functions for electron transport and carbon metabolism.

Limits and regulation of electron transport

What controls the light response of steady-state photosynthesis? To answer this question in a general way, we have extended a mechanistic framework for modeling steady-state electron transport in the C₃ case (Fig. 1a) to the C₃–C₄ and C₄ cases (Figs. 1b and c). This framework is organized around linear electron flow (LEF). In this process, light that is absorbed by PS II and PS I is used to split H₂O and drive electrons through the intersystem chain to form reductant (Fd and NADPH). Within the intersystem chain, the light-driven electron flow is coupled to proton pumping at Cyt b₆f, and the resulting proton motive force is used to drive ATP production at the ATP synthase. The Fd, NADPH, and ATP are then consumed by C₃ and/or C₄ carbon metabolism (i.e., Eqs. 1–10). Our approach to modeling LEF is based on the observation that Cyt b₆f is the primary kinetic bottleneck in the electron transport system and is the target of a hierarchy of regulatory feedbacks stemming from carbon metabolism (e.g., see reviews by Kallas 2012; Schöttler and Tóth 2014; Finazzi et al. 2016; Tikhonov 2018; Simkin et al. 2019; Malone et al. 2021; Sarewicz et al. 2021). We developed experimental methods to estimate the in vivo maximum activity of Cyt b₆f and identify the conditions under which feedback control of Cyt b₆f is active or relaxed, and then used these approaches to relate the biochemical properties

Table 2 Input parameters for C₃, Type I C₃–C₄, and C₄ simulations

Category	Symbol	Values	Units	Description
Environmental variables	Q	0–2400	umol PPFD m ⁻² s ⁻¹	Photosynthetically active radiation
	T	10–40	°C	Leaf temperature
	C_m	0–1000	μbar CO ₂	Partial pressure of CO ₂ in mesophyll chloroplasts
	O_m	209	mbar O ₂	Partial pressure of O ₂ in mesophyll chloroplasts
	P	1	bar	Total pressure
Electron transport variables	α	0.85	mol mol ⁻¹	Total leaf absorbance to PAR
	α_1/α	48, 48, 53	%	PS I fraction of total leaf absorbance
	α_2/α	52, 52, 47	%	PS II fraction of total leaf absorbance
	α_m/α	100, 95, 60	%	Mesophyll fraction of total leaf absorbance
	α_s/α	0, 5, 40	%	Bundle sheath fraction of total leaf absorbance
	$V_{max} (CB6F)$	175	μmol e ⁻ m ⁻² s ⁻¹	Maximum activity of Cyt b ₆ f
	$V_{mmax}/V_{max} (CB6F)$	100, 95, 60	%	Mesophyll fraction of Cyt b ₆ f
	$V_{smax}/V_{max} (CB6F)$	0, 5, 40	%	Bundle sheath fraction of Cyt b ₆ f
	$V_{max} (RUB)$	50, 50, 30	μmol CO ₂ m ⁻² s ⁻¹	Maximum carboxylase activity of Rubisco
	$V_{mmax}/V_{max} (RUB)$	100, 90, 0	%	Mesophyll fraction of Rubisco
Carbon metabolism variables	$V_{smax}/V_{max} (RUB)$	0, 10, 100	%	Bundle sheath fraction of Rubisco
	$V_{max} (PEPC)$	0, 0, 60	μmol CO ₂ m ⁻² s ⁻¹	Maximum activity of PEPC
	$V_{mmax}/V_{max} (PEPC)$	0, 0, 100	%	Mesophyll fraction of PEPC
	$V_{smax}/V_{max} (PEPC)$	0, 0, 0	%	Bundle sheath fraction of PEPC
	g_{bs}	0.003	mol CO ₂ m ⁻² s ⁻¹	Bundle sheath conductance to CO ₂
	R_d	0.010	%	Dark respiration scaled to V _{max} Rubisco
	K_{F1}, K_{F2}	0.05	ns ⁻¹	Rate constant for fluorescence at PS I & PS II
	K_{D1}, K_{D2}	0.55	ns ⁻¹	Rate constant for const. heat loss at PS I & PS II
	K_{P1}	14.5	ns ⁻¹	Rate constant for photochemistry at PS I
	K_{P2}	4.5	ns ⁻¹	Rate constant for photochemistry at PS II
Electron transport constants	K_{U2}	2.0	ns ⁻¹	Rate constant for excitation sharing at PS II
	k_q	300	mol PQH ₂ mol ⁻¹ sites s ⁻¹	Catalytic constant for PQH ₂ for Cyt b ₆ f
	n_L	0.75	mol ATP mol ⁻¹ e ⁻	Coupling efficiency of linear electron flow
	n_C	1.00	mol ATP mol ⁻¹ e ⁻	Coupling efficiency of cyclic electron flow
	k_c	3.6	mol CO ₂ mol ⁻¹ sites s ⁻¹	Catalytic constant for CO ₂ for Rubisco
	k_o	0.9	mol O ₂ mol ⁻¹ sites s ⁻¹	Catalytic constant for O ₂ for Rubisco
	K_c	260	μbar	Michaelis constant for CO ₂ for Rubisco
	K_o	179	mbar	Michaelis constant for O ₂ for Rubisco
	K_p	80	μbar	Michaelis constant for CO ₂ for PEPC
	D_c	1.9 · 10 ⁻⁹	m ² s ⁻¹	Diffusivity of CO ₂ in air
Carbon metabolism constants	H_c	59.4 · 10 ⁻⁵	bar ⁻¹	Solubility of CO ₂ in water
	D_o	2.4 · 10 ⁻⁹	m ² s ⁻¹	Diffusivity of O ₂ in air
	H_o	2.2 · 10 ⁻⁵	bar ⁻¹	Solubility of O ₂ in water

We have used an intentionally simplified parameterization to facilitate interpretation of the simulations. For most parameters, only a single value is given and this is applied to all three pathways. For the pathway-specific parameterizations, values are given for C₃, Type I C₃–C₄, and C₄ cases, respectively. The parameterization of constants related to carbon metabolism follows von Caemmerer (2000), and the parameterization of constants related to electron transport follows Johnson and Berry (2021). The values given for the physiological variables and all of the constants correspond to a reference temperature of 25 °C. The scaling of temperature-sensitive parameters follows the approach described in the Model Development section, where the activation term from J_{max} is assigned to V_{max} of Cyt b₆f and the deactivation term from J_{max} is assigned to the n_L and n_C parameters that describe the efficiency of coupling between NADPH, Fd, and ATP production

of Cyt b₆f to the steady-state dynamics of photosynthesis in intact C₃ leaves (Johnson and Berry 2021).

Mathematically, this framework describes the potential rate of electron transport through Cyt b₆f with a concise

analytic expression that is a rectangular hyperbolic function of incident light intensity (i.e., Eqs. 11a, b), and a linear function of the redox state of plastoquinone (Fig. 2). This form of the electron transport response to light emerges

from two regulated properties: (i) at the limit where light approaches zero, the initial slope is determined by the absorption cross-sections and maximum photochemical yields of PS I and PS II (Fig. 2a; dark-acclimated state); whereas (ii) at the limit where light goes to infinity, the asymptote is determined by the maximum activity of Cyt b₆f (Fig. 2a; V_{\max} of Cyt b₆f in mesophyll). In between these limits, the sensitivity of electron transport to light declines progressively because the light-independent kinetic bottleneck at Cyt b₆f causes an increasing fraction of the PS I and PS II reaction centers to accumulate in the closed state as the light-dependent excitation pressure on PS I and PS II increases. Due to the kinetic restriction at Cyt b₆f, the closed state is reduced at PS II and oxidized at PS I, but in both cases represents a state where photochemistry cannot occur. This creates a fundamental trade-off between the rate and the efficiency of potential electron transport through Cyt b₆f, and this trade-off structures the responses of photosynthesis to CO₂, O₂, and temperature.

As environmental conditions vary, regulatory interactions that center on Cyt b₆f maintain coordination between electron transport and carbon metabolism (e.g., see reviews by

Woodrow and Berry 1988; Foyer et al. 1990, 2012; Genty and Harbinson 1996; Baker et al. 2007; Cornic and Baker 2012; Tikkanen et al. 2012; Malone et al. 2021). For our purposes, it is sufficient to differentiate between two limiting states. We use ‘light-limited’ to refer to the metabolic state where electron transport is limiting carbon metabolism (i.e., Eqs. 11–16), and ‘light-saturated’ to refer to the metabolic state where carbon metabolism is limiting electron transport (i.e., Eqs. 17–20). Under any specific environmental condition, the actual state corresponds to the most limiting of the potential states (Fig. 2; upper bounds of green shaded regions). In the light-limited state, electron transport activity depends on the supply of substrate (reduced plastoquinone) and the V_{\max} of the rate-limiting enzyme (Cyt b₆f) (Fig. 2a–c; actual light-limited rate). Since the total light-driven electron flow is insufficient to satisfy the potential demand of the sinks for NADPH, Fd, and ATP, the activity of Rubisco and/or PEPC is downregulated to an extent that is determined by the availability of electron donors (Fig. 2a–c; blue and red shaded regions). In the light-saturated state, these patterns are reversed (Fig. 2a–c; actual light-saturated rate). Here, the activity of the sinks depends on the supply

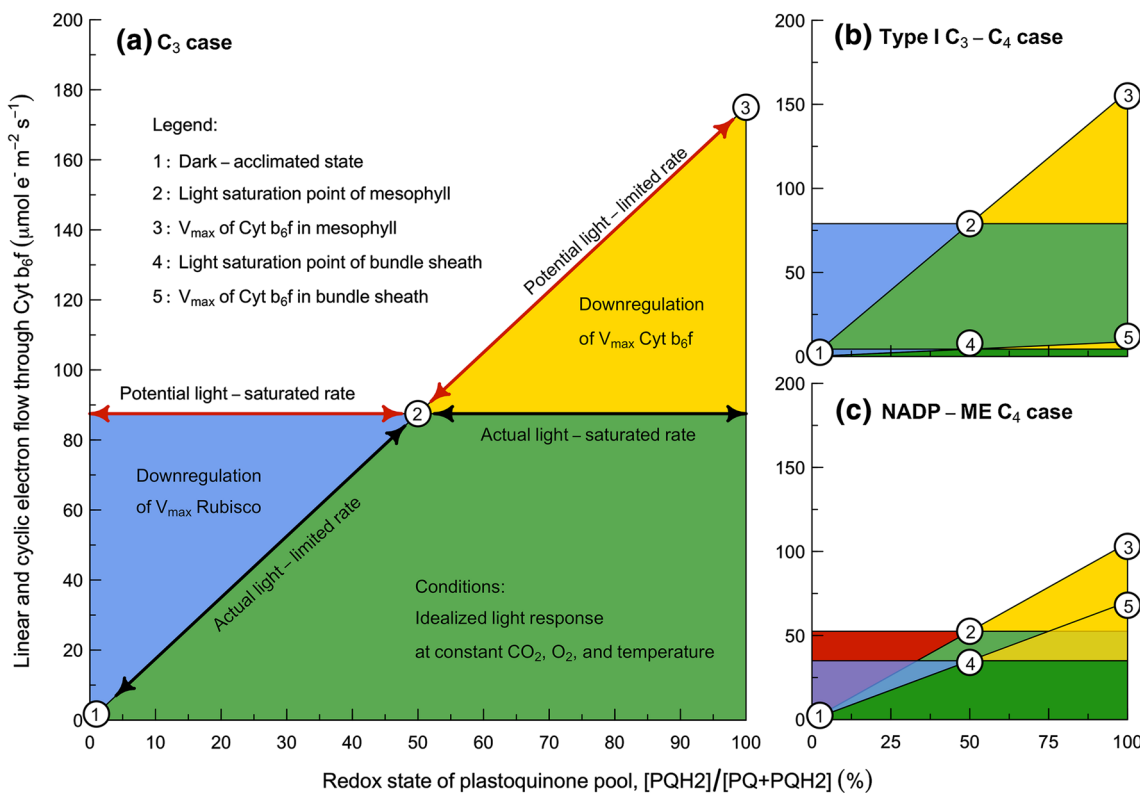


Fig. 2 The maximum activity of Cyt b₆f limits electron transport in the mesophyll and bundle sheath. For the **a** C₃, **b** Type I C₃–C₄, and **c** C₄ cases, the light-limited rates are defined by the sloping lines from the dark-acclimated state (i.e., point 1) to the V_{\max} of Cyt b₆f (i.e., point 3 in mesophyll and point 5 in bundle sheath), and the light-saturated rates are defined by the horizontal lines through the light-saturation points (i.e., point 2 in mesophyll and point 4 in bundle sheath). See text for discussions of the shaded regions. N.B., x- and y-axes are the same for all panels. LEF linear electron flow, CEF1 cyclic electron flow around PS I, PQ plastoquinone, PQH₂ plastoquinol, V_{\max} maximum activity

ration points (i.e., point 2 in mesophyll and point 4 in bundle sheath). See text for discussions of the shaded regions. N.B., x- and y-axes are the same for all panels. LEF linear electron flow, CEF1 cyclic electron flow around PS I, PQ plastoquinone, PQH₂ plastoquinol, V_{\max} maximum activity

of substrate (CO_2 and O_2) and the V_{\max} of the rate-limiting enzymes (Rubisco and/or PEPC). Since the total potential light-driven electron flow would exceed the capacity of the sinks, the activity of Cyt b₆f is downregulated to an extent that is determined by the availability of electron acceptors (Fig. 2a–c; yellow shaded regions).

The definition of the light-limited and light-saturated states permits quantification of three forms of regulation: cyclic electron flow around PS I (CEF1), non-photochemical quenching of PS II (NPQ), and photosynthetic control of Cyt b₆f (PC). In CEF1, light that is absorbed by PS I is used to drive electrons from the Fd and/or NADPH pools back into the intersystem chain and through Cyt b₆f. Since the associated proton pumping can drive ATP formation, this pathway can be engaged to balance the energy supply from electron transport with the energy demand of carbon metabolism. In the steady-state, the partitioning between LEF and CEF1 is controlled by the excitation of the PS II versus PS I antennae. As sink demands for Fd, NADPH, and ATP vary, NPQ can be engaged to adjust the excitation distribution between PS II and PS I. Different forms of NPQ can be engaged under different conditions (e.g., state transitions (qT), chloroplast movements (qM), psbS-dependent (qE) and zeaxanthin-dependent (qZ) quenching). However, the family of NPQ processes does not dissipate all of the excess excitation from the antennae system under saturating light. To protect the system from photodamage, PC can be engaged. Photosynthetic control restricts linear electron flow through Cyt b₆f to a rate that is balanced with the capacity of carbon metabolism to provide electron acceptors. Since all three of these regulatory interactions coordinate electron transport with carbon metabolism between the lumen and stroma of individual chloroplasts, they provide a foundation for analyzing how photosynthesis works when there is specialization of electron transport and carbon metabolism between populations of chloroplasts in the mesophyll and bundle sheath.

Interactions between mesophyll and bundle sheath

While chloroplasts that are experiencing similar environmental conditions and have similar photosynthetic capacities are expected to transition synchronously between light-limited and light-saturated states, chloroplasts that are experiencing dissimilar environmental conditions and/or have different photosynthetic capacities are expected to transition asynchronously between light limitation and light saturation. To model photosynthesis in a way that captures these dynamics, the equation set needs to be solved differently than has typically been done to date. The C₃–C₄ model described by von Caemmerer (2000) and the C₄ model described by von Caemmerer (2021) are based on expressions for pure states, i.e., conditions where the mesophyll

and bundle sheath are both light-limited or both light-saturated. However, since the mesophyll and bundle sheath chloroplasts are segregated in distinct environments and since each population has distinct capacities for electron transport and for carbon metabolism, the mesophyll and bundle sheath have the potential to transition independently between light-limitation and light-saturation, creating mixed states (i.e., Eqs. 21–22). The possibility of mixed states occurring within the C₄ pathway was originally hypothesized by Peisker and Henderson (1992), and it applies equally to the C₃–C₄ pathway. To simulate mixed states in a realistic way, the equation set needs to be solved in a way that respects two logical constraints: (i) the limiting state of the mesophyll controls the rate of glycine shuttling and malate shuttling to the bundle sheath, and therefore influences the bundle sheath environment, but (ii) the bundle sheath may or may not operate under the same limiting state as the mesophyll. To achieve this, we have developed a hierarchical approach to solving the equation set (i.e., Eqs. 23–25).

To evaluate the hierarchical solution, we tested the skill of the full model in simulating the light response of the CO₂ compensation point (Γ). The CO₂ compensation point is defined as the CO₂ concentration at which there is no net CO₂ assimilation. The Γ values of C₃ and C₄ plants are nearly insensitive to light intensity, with the exception being at very low light intensities where there is a respiratory effect (Laing et al. 1974; Čatský and Tichá 1979; Peisker 1979; Farquhar et al. 1980a; Brooks and Farquhar 1985). In the C₃ case, Γ corresponds to a state where the CO₂ uptake driven by Rubisco carboxylase activity is balanced by the CO₂ loss driven by Rubisco oxygenase activity and mitochondrial (dark) respiration (i.e., from Eq. 5, $V_{cm} = V_{gm} + R_m$). In the C₄ case, Γ corresponds to a state where the CO₂ uptake driven by PEPC in the mesophyll is balanced by the CO₂ loss driven by the diffusive leak out of the bundle sheath (i.e., from Eq. 5, $V_{pm} = L + R_m$). In these cases, the activities of Rubisco and PEPC are kinetically limited by the CO₂ supply rather than energetically limited by electron transport, such that Γ is insensitive to light intensity. In contrast, the Γ values of C₃–C₄ plants decrease curvilinearly in response to increasing light intensities (Brown and Morgan 1980; Holaday et al. 1982; Hattersley et al. 1986; Rajendrudu et al. 1986; Cheng et al. 1989; Ku et al. 1991; Dai et al. 1996). The oxygen and temperature responses of the Γ values of C₃–C₄ plants also appear to be sensitive to light intensity, with higher light intensities associated with higher breakpoints in each response (Keck and Ogren 1976; Quebedeaux and Chollet 1977; Apel 1980; Morgan and Brown 1980; Brown and Morgan 1980; Holaday et al. 1982, 1984; Hunt et al. 1987; Moore et al. 1987a; Ku et al. 1991; Dai et al. 1996; Vogan et al. 2007). To date, it has not been clear what mechanisms are responsible for the environmental responses of Γ in C₃–C₄ plants, but mixed states seem likely to be

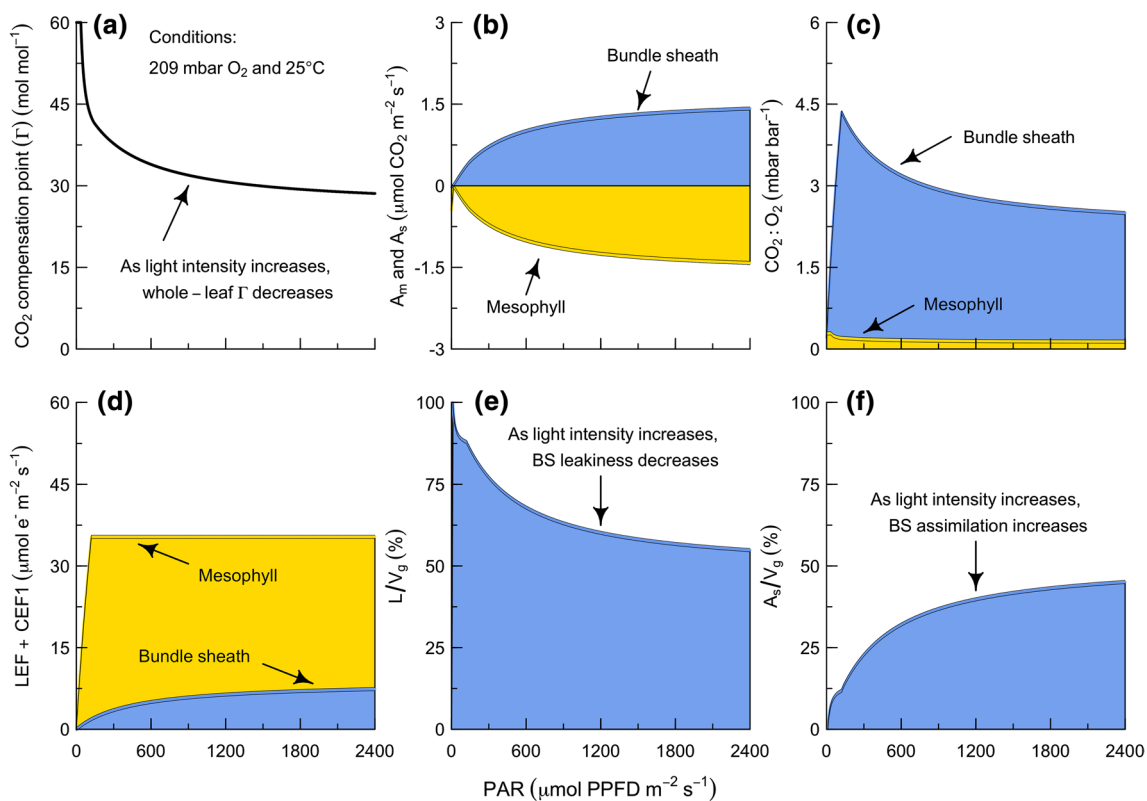


Fig. 3 Photosynthetic control of Cyt b₆f occurs independently in the mesophyll and bundle sheath. To simulate the light dependence of the CO₂ compensation point (Γ) in the Type I C₃–C₄ intermediate pathway, the model must be solved in a way that permits each cell type to transition independently between the limiting states. See text for details of each panel. N.B., x-axes are the same for all panels. A_m

and A_s , net rates of CO₂ assimilation in mesophyll and bundle sheath. LEF linear electron flow, CEF1 cyclic electron flow around PS I, L rate of CO₂ leak from bundle sheath via diffusion, V_g rate of CO₂ delivery to bundle sheath via glycine shuttle, PAR photosynthetically active radiation

involved (Edwards and Ku 1987; Rawsthorne et al. 1992; Rawsthorne 1992; Leegood and von Caemmerer 1994; von Caemmerer 2000).

The model predicts that a pure state is responsible for the light-insensitive values of Γ in the C₃ and C₄ cases (i.e., 47 and 0.5 μbar CO₂ at 25 °C, respectively), and that a mixed state is responsible for the light-sensitivity of Γ in the Type I C₃–C₄ case (Fig. 3a). Here, Γ corresponds to a state where the CO₂ uptake driven by Rubisco carboxylase activity in the mesophyll is equivalent to the CO₂ loss driven by the diffusive leak out of the bundle sheath (i.e., from Eq. 5, $V_{cm}=L+R_m$). At this point, the mesophyll is a net CO₂ source and the bundle sheath is a net CO₂ sink (Fig. 3b). The mesophyll is a net CO₂ source because the glycine shuttle is mobilizing fixed carbon from the mesophyll and delivering the derived CO₂ to the bundle sheath. The bundle sheath is a net CO₂ sink because the bundle sheath CO₂ is raised to a level that permits net export of reduced carbon from the bundle sheath Rubisco population. When the mesophyll and bundle sheath are both light-limited, increasing light stimulates CO₂ delivery to and uptake within the bundle

sheath. However, the CO₂ delivery to the bundle sheath increases faster than the CO₂ uptake within the bundle sheath, such that the CO₂:O₂ ratio rises (Fig. 3c). Since this also increases the rate at which CO₂ leaks out of the bundle sheath, Γ would stabilize if the mesophyll and bundle sheath were both to remain light-limited. Instead, the CO₂ supply to the bundle sheath stabilizes when the mesophyll becomes light-saturated (Fig. 3d). While the bundle sheath remains light-limited, the activity of Rubisco continues to be stimulated by light, drawing down the CO₂:O₂ ratio in the bundle sheath and slowing the rate at which CO₂ leaks out of the bundle sheath (Fig. 3e). The net effect of these interactions is that a larger fraction of the CO₂ delivered to the bundle sheath is assimilated, such that Γ continues to decrease with light (Fig. 3f). Based on this analysis, we conclude that the light-sensitivity of Γ is most likely an indicator of a mixed state. Mixed states are likely to be a key component of C₃–C₄ photosynthesis as well as C₄ photosynthesis. They may be encountered either when leaves are exposed to environmental conditions that are outside those they have acclimated

to during growth (e.g., such as Γ), or under normal growth conditions (e.g., during parts of the diel cycle).

Basis of temperature sensitivities

While the Cyt b₆f-based description of electron transport and the mixed state solution permit the model to simulate the response of photosynthesis to variation in light, CO₂, and O₂ under constant temperature, additional expressions are required to explain the temperature-dependence of photosynthesis. At present, several different functions are in use and many species-specific parameter sets have been derived for each of them (e.g., see Berry and Raison 1981; Sellers et al. 1996b; von Caemmerer 2000; von Caemmerer et al. 2009; Bernacchi et al. 2013). In principle, any of these expressions can be applied to this model. However, the fundamental challenge in choosing among these functions is neither the appropriate functional form nor the correct parameter values, but the assignment of scaling factors to the correct underlying mechanisms. In particular, it is not yet clear how the intrinsic temperature sensitivities of the electron transport system interact with the intrinsic temperature sensitivities of carbon metabolism. The primary observations that are relevant to this question are: (i) LEF usually exhibits a thermal optimum and declines at high temperatures (e.g., Yamori et al. 2014); (ii) CEF1 is usually stimulated relative to linear electron transport at high temperatures (e.g., Ivanov et al. 2017); (iii) NPQ tends to be stimulated at high temperatures (e.g., Demmig-Adams et al. 2014); (iv) the plastoquinone pool tends to become more oxidized at high temperatures (e.g., Sharkey and Zhang 2010); and (v) the turnover constant of Cyt b₆f tends to increase with temperature (e.g., Tikhonov 2018). However, it has been difficult to understand the basis of these effects due to the close coordination between the activity of the electron transport system and of carbon metabolism. It has been proposed both that the activity of Rubisco is downregulated at high temperatures due to a limitation on the activity of the electron transport system, and that the activity of the electron transport system is downregulated at high temperatures due to a limitation on the activity of Rubisco.

To compare the various alternatives quantitatively, we have parameterized the new model with different combinations of the temperature sensitivities that Farquhar et al. (1980a) originally assigned to electron transport through the empirical parameter J_{\max} (Fig. 4). For all of the simulations, we have maintained a fixed set of temperature responses for carbon metabolism (i.e., following Farquhar et al. 1980a as reviewed by von Caemmerer et al. 2009). Within this background, we have selectively varied the localization of the activation and deactivation terms from J_{\max} (E_a of 37 kJ mol⁻¹, H_d 220 kJ mol⁻¹, ΔS 0.710 kJ mol⁻¹ K⁻¹). The alternative localizations are: (1) no assignment of the J_{\max}

coefficients; (2) J_{\max} activation term on V_{\max} of Cyt b₆f; (3) J_{\max} activation and deactivation terms on V_{\max} of Cyt b₆f; (4) J_{\max} activation term on V_{\max} of Cyt b₆f and deactivation terms on V_{\max} of Rubisco; (5) J_{\max} activation term on V_{\max} of Cyt b₆f and deactivation terms on the efficiency of coupling between electron transport and ATP production. While all five parameterizations predict a thermal optimum in net CO₂ assimilation (Fig. 4a), each predicts a distinct combination of temperature responses in the rate of LEF (Fig. 4b), the rate of CEF1 (Fig. 4c), the level of NPQ of PS II (Fig. 4d), the redox poise of the plastoquinone pool (Fig. 4e), and the turnover constant of Cyt b₆f (Fig. 4f). The predictions only capture all of the primary features of the observations when the activation term from J_{\max} is assigned to V_{\max} of Cyt b₆f and the deactivation term from J_{\max} is assigned to the n_L and n_C parameters that describe the efficiency of coupling between NADPH, Fd, and ATP production (Fig. 4b–f; red lines). This suggests that increasing temperatures may have two general effects on the electron transport system: first, increasing the V_{\max} of Cyt b₆f; and second, decreasing the efficiency of coupling between NADPH, Fd, and ATP production.

These results have three main implications. First, this modeling framework provides a new foundation for understanding and predicting the temperature responses of photosynthesis. In this analysis, we have leveraged existing temperature response functions to illustrate the model's ability to simulate multiple observable quantities derived from gas-exchange, fluorescence, and absorbance measurements. However, this application should not be interpreted as an endorsement either of this specific functional form or this specific parameterization. Further research is needed to evaluate the most appropriate functional form and parameterization of the temperature responses. Second, it is likely that increasing temperature stimulates the maximum activity of Cyt b₆f, but the magnitude of this effect is in need of improved quantification. Although assigning the activation term from J_{\max} to V_{\max} of Cyt b₆f permits a qualitatively realistic simulation of the temperature response, this is not expected to be quantitatively realistic because the V_{\max} of Cyt b₆f is not equivalent to the J_{\max} parameter of Farquhar et al. (1980a). The J_{\max} parameter represents the rate of electron transport that occurs under saturating light and saturating CO₂, and in C₃ leaves at 25 °C this is around one-half of the true maximum potential rate of electron transport that is defined by the substrate-saturated rate of electron flow through Cyt b₆f (Johnson and Berry 2021). In vivo and in vitro evaluations of the temperature sensitivity of the V_{\max} of Cyt b₆f are needed. Third, the reversible decline in photosynthesis at high temperatures may be caused by a decline in the efficiency of coupling between NADPH, Fd, and ATP production. In principle, such a decline in coupling efficiency might be driven by

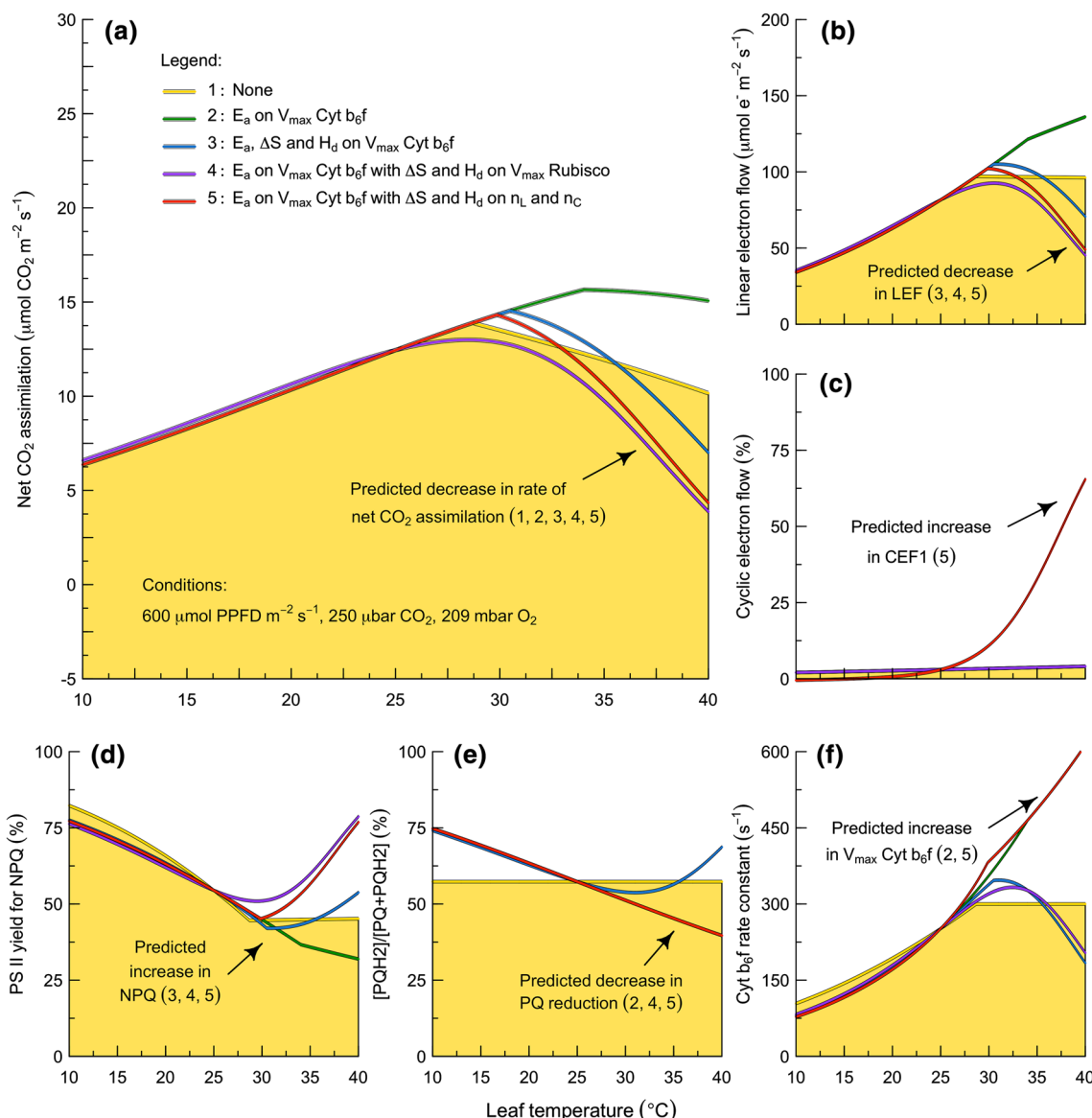


Fig. 4 The contributions of Cyt b₆f and the coupling efficiency to the temperature response of photosynthesis. These simulations examine C₃ photosynthesis. Yellow shading indicates the reference where the temperature response is driven by carbon metabolism alone. The fifth simulation captures all of the physiological responses that are typi-

cally observed. See text for details. N.B., x-axes are the same for all panels. E_a enthalpy of activation (37 kJ mol^{-1}), H_d enthalpy of deactivation (220 kJ mol^{-1}), ΔS entropy factor (0.710 $\text{kJ mol}^{-1} \text{ K}^{-1}$). LEF linear electron flow, CEF1 cyclic electron flow around PS I, NPQ non-photochemical quenching, PQ plastoquinone, PQH₂ plastoquinol

a temperature effect on: (i) the coupling between electron flow and proton translocation at Cyt b₆f; (ii) the proton “leakiness” of the thylakoid membrane; (iii) the coupling between proton translation and ATP formation at ATP synthase; and/or (iv) other related mechanisms. This possibility is distinct from the alternative hypotheses that are currently dominant, and the full range of hypotheses deserve careful experimental evaluation. In the next section, we will illustrate how the model can be used as a tool to aid in this type of quantitative interpretation of physiological measurements.

Model applications

This model can be used for forward simulations and for inverse fitting. In this section, we provide examples of both types of applications. We first present forward simulations that illustrate the responses of C₃, Type I C₃–C₄, and C₄ photosynthesis to light, carbon dioxide, and temperature. The simulations demonstrate how the Cyt b₆f-based expressions for electron transport, the hierarchical solution for mixed states, and the temperature dependencies come together in the overall performance of the model. We then

present inverse analyses that illustrate how the model can be used to interpret gas-exchange measurements of a Type I C₃–C₄ plant, *Flaveria chloraeifolia*. The inverse analyses demonstrate that population-level variation in the CO₂ compensation point in this species can be explained by variable allocation of photosynthetic capacity to the bundle sheath. We conclude by discussing key questions that are raised by this framework and posing a novel hypothesis about the origins of C₄ photosynthesis.

Forward simulations

The responses of photosynthesis to light, carbon dioxide, and temperature vary substantially between the C₃, Type I C₃–C₄, and C₄ pathways (Fig. 5a–c). Part of the variation is controlled by pathway- and cell-type-specific differences in photosynthetic capacity which control the absolute amounts of Fd, NADPH, and ATP produced and consumed (Table 2). The remainder of the variation is controlled by pathway- and cell-type-specific differences in photosynthetic metabolism which control the relative amounts of Fd, NADPH, and ATP that are produced and consumed (Appendix I: Electronic Supplementary Material). In this model, three forms of regulation coordinate the energy supply from electron transport with the energy demand from carbon metabolism. In any given pathway and cell type, the flux through LEF versus CEF1 is dynamically modulated to establish a sink-appropriate balance between the supply of ATP and the supply of Fd and NADPH (Fig. 5d–f). The partitioning between LEF and CEF1 is controlled by the distribution of excitation between PS I and PS II. This depends on the relative absorption cross-section of each population of photosynthetic units and the level of connectivity between photosynthetic units, and is dynamically modulated through NPQ (Fig. 5g–i). Once the energy supply and demand are balanced in relative terms, the final requirement is ensuring that they are also balanced in absolute terms. This is achieved via PC of Cyt b₆f, which restricts the rate of electron flow to the capacity of carbon metabolism to provide acceptors (Fig. 5j–l). Across the three pathways, PC tends to be relaxed at low light and to become engaged as the light intensity is increased (Fig. 5j), to be engaged at low CO₂ and to relax as the CO₂ concentration is increased (Fig. 5k), and to be engaged at low temperature and to relax as the temperature is increased (Fig. 5l). However, the Type I C₃–C₄ bundle sheath remains light-limited under all of these conditions, and the C₄ mesophyll remains light-limited under most conditions except the lowest CO₂ concentrations and lowest temperatures. As a result, mixed states are common in both the Type I C₃–C₄ and C₄ pathways along all three environmental axes.

These simulations demonstrate that this framework both reproduces the core dynamics of earlier photosynthesis

models and introduces new capabilities with respect to the interactions between the light, CO₂, and temperature responses. To date, the expressions for light-saturated photosynthesis that were summarized by von Caemmerer (2000) have been successful at reproducing: (i) a CO₂ compensation point for C₃–C₄ plants that is intermediate to those of C₃ and C₄ plants at atmospheric O₂ levels; (ii) a non-linear response of the CO₂ compensation point to variation in O₂ in C₃–C₄ plants; and (iii) a curvilinear response of net CO₂ assimilation to variation in CO₂ in C₃ and C₃–C₄ plants, as well as a biphasic response in C₄ plants. The framework we have described here builds on this foundation by introducing expressions for light-limited photosynthesis that are successful at reproducing: (iv) a curvilinear response of net CO₂ assimilation to variation in light in C₃, C₃–C₄, and C₄ plants; (v) a CO₂ compensation point that is light-dependent in C₃–C₄ plants; and (vi) a light-dependent decline in net CO₂ assimilation at high temperatures in C₃, C₃–C₄, and C₄ plants. Compared to the empirical expressions that are currently used to describe the light response, this more mechanistic approach has two main advantages: it provides a clearer interpretation of how photosynthesis works as an interactive system, and it provides a stronger connection to quantities that are directly observable. For example, the model enables analysis of the flux of light available to the mesophyll vs. bundle sheath (i.e., a function of the absorptance of each chloroplast population), and the light saturation point of the mesophyll vs. bundle sheath (i.e., a function of the balance between the Cyt b₆f and Rubisco in each chloroplast population). These limits are quite important because they structure the suite of regulatory interactions that coordinate electron transport with carbon metabolism (e.g., Fig. 5). However, at present there is relatively little quantitative understanding of how pigment and protein distributions vary within and between C₃, Type I C₃–C₄, and C₄ plants. In the next section, we turn to inverse fitting to explore pigment and protein distributions and their functional consequences.

Inverse fitting

By fitting the model to observations within an inversion framework, the total amounts of pigment and protein as well as the relative allocation of pigment and protein to the bundle sheath can be inferred rather than prescribed. As an example of this approach, we have applied the model to the interpretation of the photosynthetic performance of *Flaveria chloraeifolia* (Asteraceae). *F. chloraeifolia* is a Type I C₃–C₄ species that has been grown and studied under controlled conditions for decades (e.g., Powell 1978; Holaday et al. 1984; Holaday and Chollet 1984; Reed and Chollet 1985; Bauwe and Chollet 1986; Edwards and Ku 1987; Chastain

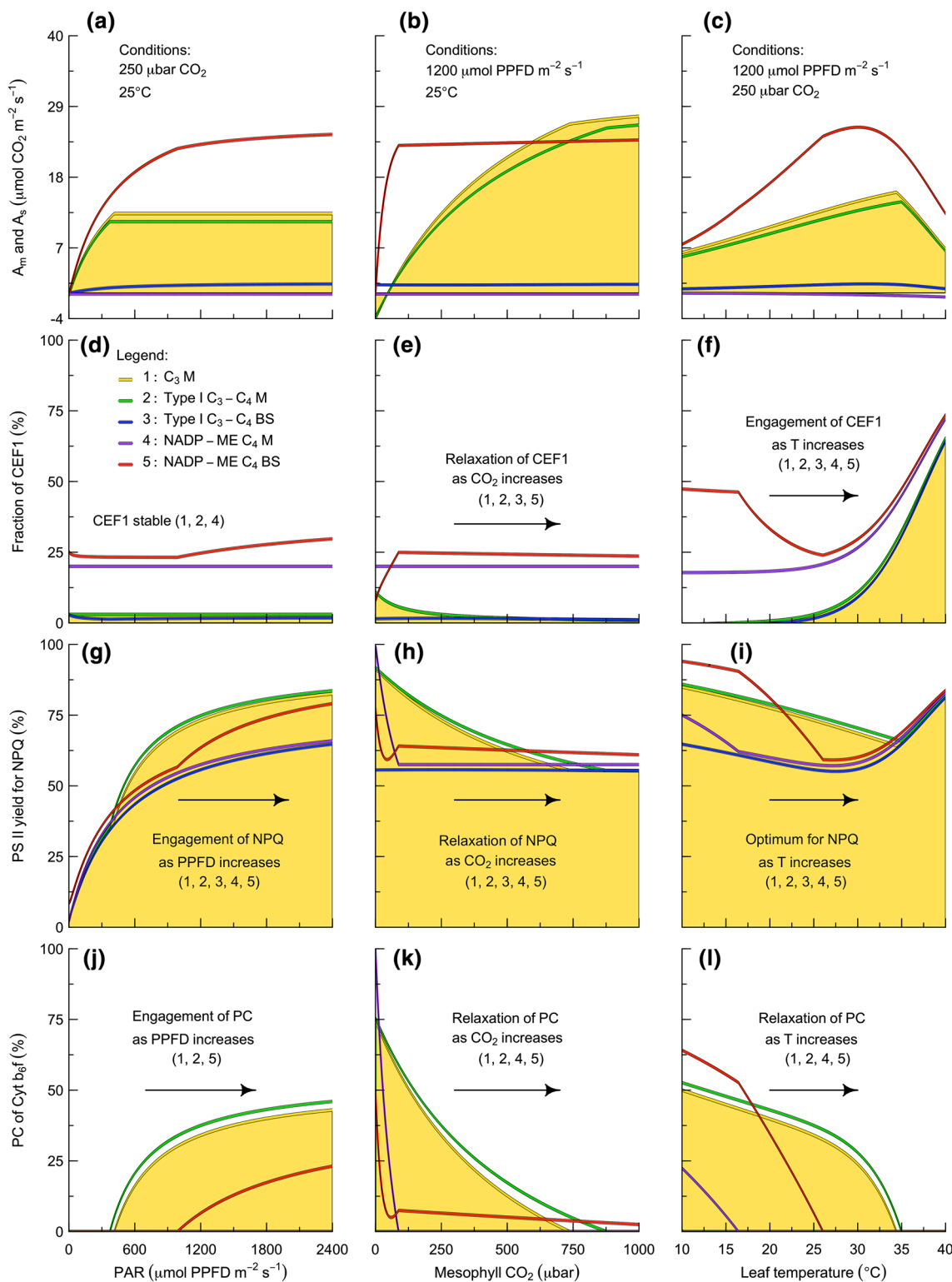


Fig. 5 Responses of C₃, Type I C₃–C₄, and C₄ photosynthesis to light, carbon dioxide, and temperature. For each environmental variable, simulations are plotted separately for C₃ mesophyll, Type I C₃–C₄ mesophyll and bundle sheath, and NADP-ME C₄ mesophyll and bundle sheath. In each plot, yellow shading indicates the reference simulation that corresponds to the C₃ case. Parameters are as in Table 2.

See text for other details. N.B., x-axes are the same for panels in each column. LEF linear electron flow, CEF1 cyclic electron flow around PS I, NPQ non-photochemical quenching of PS II, PC photosynthetic control of Cyt b₆f, M mesophyll, BS bundle sheath, PAR photosynthetically active radiation

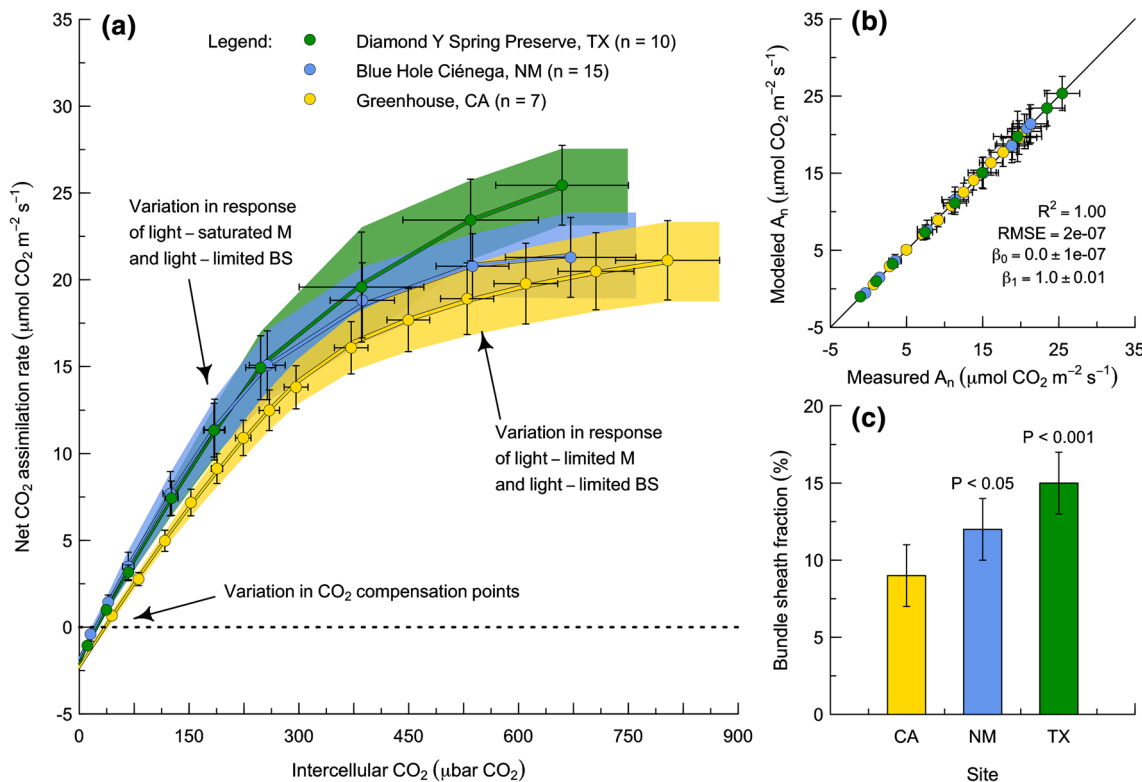


Fig. 6 Patterns and determinants of photosynthetic performance in *Flaveria chloraeefolia* (Type I $\text{C}_3\text{-}\text{C}_4$) at three sites in different environments. **a** At each site, the CO_2 response of photosynthesis was assayed between 0 and 1000 $\mu\text{bar CO}_2$ at 1500 $\mu\text{mol PPFD m}^{-2} \text{ s}^{-1}$, 27.5 to 32.5 $^{\circ}\text{C}$, and 210 mbar O_2 using a LI-6400XT (LI-COR, Lin-

coln, NE) (points). The photosynthesis model was then fit to each individual CO_2 response (lines). **b** The model fit the measurements well, without any bias and with little noise. **c** There was significant variation between sites in the fraction of total absorptance. V_{\max} of Cyt b₆f, and V_{\max} of Rubisco in the bundle sheath. See text for details

and Chollet 1989; Ku et al. 1991; Dai et al. 1996; Kopriva et al. 1996; Pfundel and Pfeffer 1997; Leonards and Grodzinski 2000, 2003; Engelmann et al. 2003; Huxman and Monson 2003; Westhoff and Gowik 2004; McKown et al. 2005; McKown and Dengler 2007; Kocacinar et al. 2008; Vogan and Sage 2011; Schulze et al. 2013; Aldous et al. 2014; Mallmann et al. 2014; Way et al. 2014; Stata et al. 2016; Lyu et al. 2021). However, there are very few studies of this species under field conditions (e.g., Van Auken et al. 2007; Peralta-García et al. 2016; Ochoterena et al. 2020; Peralta-García et al. 2020; Pisanty et al. 2020; Rodríguez-Sánchez et al. 2020). We compared the photosynthetic performance of a greenhouse-grown research population at the Carnegie Institution in Stanford, CA to that of naturally-occurring populations at the Blue Hole Ciénega in Guadalupe County, NM ($34^{\circ} 56' 8'' \text{ N}, 104^{\circ} 40' 30'' \text{ W}$), and the Diamond Y Spring Preserve in Pecos County, TX ($31^{\circ} 0' 36'' \text{ N}, 102^{\circ} 55' 5'' \text{ W}$). Measurements of the CO_2 response of mature leaves were made on the research population in CA during the mid-winter, and on the wild populations in NM and TX during the mid-summer. At each site, measurements were made for $n = 7\text{--}15$ individual leaves. For each leaf,

a LI-6400XT (LI-COR, Lincoln, NE) system was used to vary CO_2 from 0 to 1000 μbar , at 210 mbar O_2 , with a light intensity of 1500 $\mu\text{mol PPFD m}^{-2} \text{ s}^{-1}$ and leaf temperatures ranging between 28 and 33 $^{\circ}\text{C}$.

To interpret the basis of the measured responses, we fit each individual CO_2 response curve to the model using an optimization framework (Fig. 6). Tests with synthetic data that mimicked the real sampling design and error characteristics demonstrated that the fitting procedure could be expected to retrieve up to four free parameters to within $\pm 1\%$ of their true values. The four free variables we selected for fitting were: (i) mesophyll conductance to CO_2 , (ii) V_{\max} of Cyt b₆f, (iii) V_{\max} of Rubisco, and (iv) the fraction of the total absorptance, V_{\max} of Cyt b₆f and V_{\max} of Rubisco in the bundle sheath. In the measurements, there was leaf-to-leaf variation in three aspects of the CO_2 response: (i) the sensitivity of net CO_2 assimilation to CO_2 at high intercellular CO_2 ; (ii) the sensitivity of net CO_2 assimilation to CO_2 at low intercellular CO_2 ; and (iii) the CO_2 compensation point (Fig. 6a; points). The largest differences were between the greenhouse-grown research population in CA and the two wild populations in NM and TX. Compared

Table 3 Parameter estimates for *Flaveria chloraeifolia* (Type I C₃–C₄) in CA, NM, and TX

Parameters	Parameter estimates: 50th (25th, 75th)			Pairwise comparisons		
	CA	NM	TX	CA:NM	CA:TX	NM:TX
g_m (mol CO ₂ m ⁻² s ⁻¹)	0.28 (0.19, 0.36)	0.40 (0.33, 0.48)	0.35 (0.22, 0.47)	$P > 0.050$	$P > 0.050$	$P > 0.050$
V_{max} Cyt b ₆ f (μmol e ⁻ m ⁻² s ⁻¹)	117 (98, 137)	133 (120, 146)	193 (146, 240)	$P > 0.050$	$P < 0.001$	$P = 0.001$
V_{max} Rubisco (μmol CO ₂ m ⁻² s ⁻¹)	52 (41, 63)	61 (55, 67)	59 (51, 67)	$P > 0.050$	$P > 0.050$	$P > 0.050$
Bundle sheath allocation (%)	9 (7, 11)	12 (10, 14)	15 (13, 17)	$P = 0.044$	$P < 0.001$	$P = 0.018$

The fitting procedure estimated four free variables. Mesophyll conductance to CO₂ was treated as a temperature-invariant parameter. The maximum activities for Cyt b₆f and Rubisco were scaled from the measurement temperatures to a reference temperature of 25 °C. The bundle sheath allocation was treated as a single parameter representing fractional allocation of absorptance, Cyt b₆f, and Rubisco to the bundle sheath. Pairwise comparisons were performed using *t* tests

to the greenhouse-grown/laboratory-measured population, the naturally-occurring/field-measured populations tended to exhibit higher sensitivities of net CO₂ assimilation to CO₂ across the entire sampled range as well as lower CO₂ compensation points. The model was able to fit these patterns by varying the mesophyll conductance to CO₂, the total amounts of Cyt b₆f and Rubisco, and the fractional allocations of the total absorptance, V_{max} of Cyt b₆f and V_{max} of Rubisco to the bundle sheath (Fig. 6a; lines and shaded confidence intervals). The fits did not exhibit any systematic biases and had relatively little noise (Fig. 6b). Within each of the three populations, there was some leaf-to-leaf variation in mesophyll conductance to CO₂, V_{max} of Cyt b₆f, and V_{max} of Rubisco (Table 3). However, the parameter that exhibited the largest systematic variation between the three populations was the bundle sheath fraction of absorptance, Cyt b₆f, and Rubisco (i.e., with a range from 7 to 17%; Fig. 6c; Table 3).

These results have three notable features. First, the quality-of-fit statistics indicate that the model structure is formulated in a way that captures the major features of the measurements. This is significant because it suggests that model parameterization, rather than model structure, could be the primary factor contributing to the long-standing discrepancy between the predicted versus observed performance of Type I C₃–C₄ plants (i.e., why they have not exhibited higher rates of net CO₂ assimilation than C₃ plants under saturating light, moderate leaf temperatures, and modern atmospheric CO₂ and O₂ levels; as discussed in the Introduction). Specifically, in previous applications of the modeling framework described by von Caemmerer (2000), the parameterizations of C₃ and Type I C₃–C₄ simulations have assumed equivalent photosynthetic capacities. This may be unrealistic, and leads to the second point: the ranges of variation in the estimated values of mesophyll conductance to CO₂, V_{max} of Cyt b₆f, and V_{max} of Rubisco are limited. The restricted ranges could reflect underlying anatomical constraints which facilitate the operation of the glycine shuttle, such as

contact between mesophyll and bundle sheath cells. This is significant because it indicates that realizing the biochemical advantages of the glycine shuttle may entail an anatomical trade-off, and such a trade-off could help to reconcile observations of Type I C₃–C₄ physiology with current understanding of the glycine shuttle. For example, if C₃–C₄ plants are restricted to a limited range of specific leaf areas, this could limit the range of V_{max} values of Cyt b₆f and Rubisco below that of C₃ plants and help to explain lower area-based measurements of the rate of net CO₂ assimilation. Third, the bundle sheath fraction of absorptance, Cyt b₆f, and Rubisco not only varies significantly between populations, but also is consistently higher in the wild populations in NM and TX than in the greenhouse-grown population in CA. This indicates that the allocation of photosynthetic capacity to the bundle sheath is flexible, and suggests that C₃–C₄ intermediate plants optimize pigment and protein distributions to maximize the benefits and minimize the costs of glycine shuttling in different environments. In combination, these findings demonstrate the potential of the inversion-based approach to the interpretation of physiological measurements. Developing this approach further requires revisiting the quantitative definition of the energetics of glycine shuttling. This is the topic we turn to in the final section.

Key questions

The structure of the Type I C₃–C₄ model we have implemented here is a quantitative expression of a conceptual model in which the confinement of glycine decarboxylation to the bundle sheath has only one functional consequence: under conditions that promote oxygen fixation by mesophyll Rubisco, glycine is transported into the bundle sheath and the CO₂ released from bundle sheath GDC activity builds up, increasing the bundle sheath CO₂/O₂ ratio and increasing the efficiency of CO₂ fixation by the bundle sheath Rubisco. Several independent lines of evidence support the inference that confinement of GDC activity to the bundle sheath

drives diffusive transport of glycine into the bundle sheath (Rawsthorne and Hylton 1991; Leegood and von Caemmerer 1994) and increases the efficiency of CO₂ fixation by the bundle sheath Rubisco (Moore et al. 1987b; Keerberg et al. 2014). However, the activity of GDC is coordinated with the activity of serine hydroxymethyl transferase such that the overall products of glycine decarboxylation include serine, NH₃, and NADH, in addition to CO₂ (Woo and Osmond 1976; Sarojini and Oliver 1983). While this implies that serine, NH₃, NADH, and/or stoichiometrically equivalent products of their metabolism must return from the bundle sheath to the mesophyll, it is not yet clear which mechanisms maintain carbon, nitrogen, and redox balance (Rawsthorne et al. 1988a, 1992; Leegood and von Caemmerer 1994; Mallmann et al. 2014; Schlüter et al. 2017).

Since NH₃ can escape to the atmosphere (Farquhar et al. 1980b; Johnson and Berry 2013), it seems likely that it is reassimilated in the bundle sheath via glutamine synthetase and/or glutamate synthase (Rawsthorne et al. 1988b, 1992; Monson and Rawsthorne 2000). If this occurs, then the glycine shuttle could either: (i) create an additional ATP demand in the bundle sheath (i.e., NH₃ reassimilated in bundle sheath chloroplasts by glutamine synthetase alone); and/or (ii) create an additional ATP, NADPH, and Fd demand in the bundle sheath (i.e., NH₃ reassimilated in bundle sheath chloroplasts by glutamine synthetase and glutamate synthase). In theory, these energetic demands could potentially be satisfied by several different energy-balancing mechanisms: (iii) a shift in the balance of linear and cyclic electron flow within the bundle sheath chloroplasts; (iv) a shift in the balance of NADH oxidation via the malate valve, cytochrome oxidase, and alternative oxidase pathways within the bundle sheath mitochondria; and/or (v) shuttling of 3-phosphoglyceric acid and dihydroxyacetone phosphate between the bundle sheath and mesophyll. Considering the range of candidate mechanisms from a stoichiometric perspective indicates that there is potential for interactions between the fate of NH₃ and the fate of NADH within the glycine shuttle, and also for interactions between the glycine, aspartate, and malate shuttles (e.g., Mallmann et al. 2014; Bellasio 2017; Schlüter and Weber 2020). However, it is not yet clear which of these interactions actually play out.

To explore the ecological context for these biochemical interactions, we parameterized the photosynthesis model with the fitted values of the physiological variables from the Diamond Y Spring Preserve (Table 3) and then simulated Type I C₃–C₄ photosynthesis at this site over one day in July (Fig. 7). For simplicity, the leaf temperature was prescribed as equivalent to air temperature, and mesophyll CO₂ and O₂ were prescribed as 250 µbar and 210 mbar, respectively (i.e., omitting the dynamic coupling between photosynthesis, stomatal conductance, and the energy balance). All

other input parameters were as given in Table 2. With this approach, the diel cycle of light and temperature (Fig. 7a) determines the limits of the potential rates of electron transport (Fig. 7b). From these limits, CEF1 (Fig. 7c), NPQ of PS II (Fig. 7d), and PC of Cyt b₆f (Fig. 7e) then regulate the actual linear electron flow to a rate that remains coordinated with the capacity of carbon metabolism to provide electron acceptors (Fig. 7f). These dynamics illustrate both challenges and opportunities for bundle sheath assimilation of NH₃ via glutamine synthetase and/or glutamate synthase. In particular, the small fractional allocation of photosynthetic capacity to the bundle sheath implies that reassimilation of mesophyll-derived NH₃ would be likely to dominate the bundle sheath energy budget. While the increased ATP to Fd and NADPH ratio associated with glutamine synthetase activity could potentially be met through increased CEF1, it could also be limited by decreased coupling efficiency at high temperatures. Alternatively, a decreased coupling efficiency might permit the chloroplast chain to support the increased Fd and NADPH to ATP ratio associated with glutamate synthase activity. In either case, the bundle sheath would be likely to make the most efficient use of the available light under conditions where state transitions optimize the absorption cross-sections of PS I and PS II (i.e., without wasting absorbed light through the heat-dissipating forms of non-photochemical quenching) such that electrons flow to the sink at the maximum possible rate (i.e., without inducing PC of Cyt b₆f).

In this context, it is intriguing to consider whether the malate and aspartate shuttles might have originally functioned to smooth out the energy supply and demand associated with the glycine shuttle, and thereby to maintain the bundle sheath in an energetically balanced state. If this is the case, it would imply that the CO₂-concentrating function of the malate and aspartate shuttles was not the reason for their origin (i.e., much like the spandrels of San Marco; Gould and Lewontin 1979). Such a hypothesis can be explored quantitatively if the chloroplast and mitochondrial electron transport chains are conceptualized as part of a single, interactive system that balances energy supply and demand, subject to the inherent kinetic limits of each chain and the manner in which they are regulated. The model we have described here provides a framework for performing this type of analysis and determining which combinations of potential interactions actually operate in vivo in different plants and under different environmental conditions. Since *Flaveria chloraeifolia* co-exists with C₃ and C₄ competitors at the Diamond Y Spring and the Blue Hole Ciénega, further study of these communities may provide insight into the mechanisms of competitive coexistence and whether the ecological conditions here allow the Type I C₃–C₄ pathway to represent an evolutionarily stable strategy. In a global

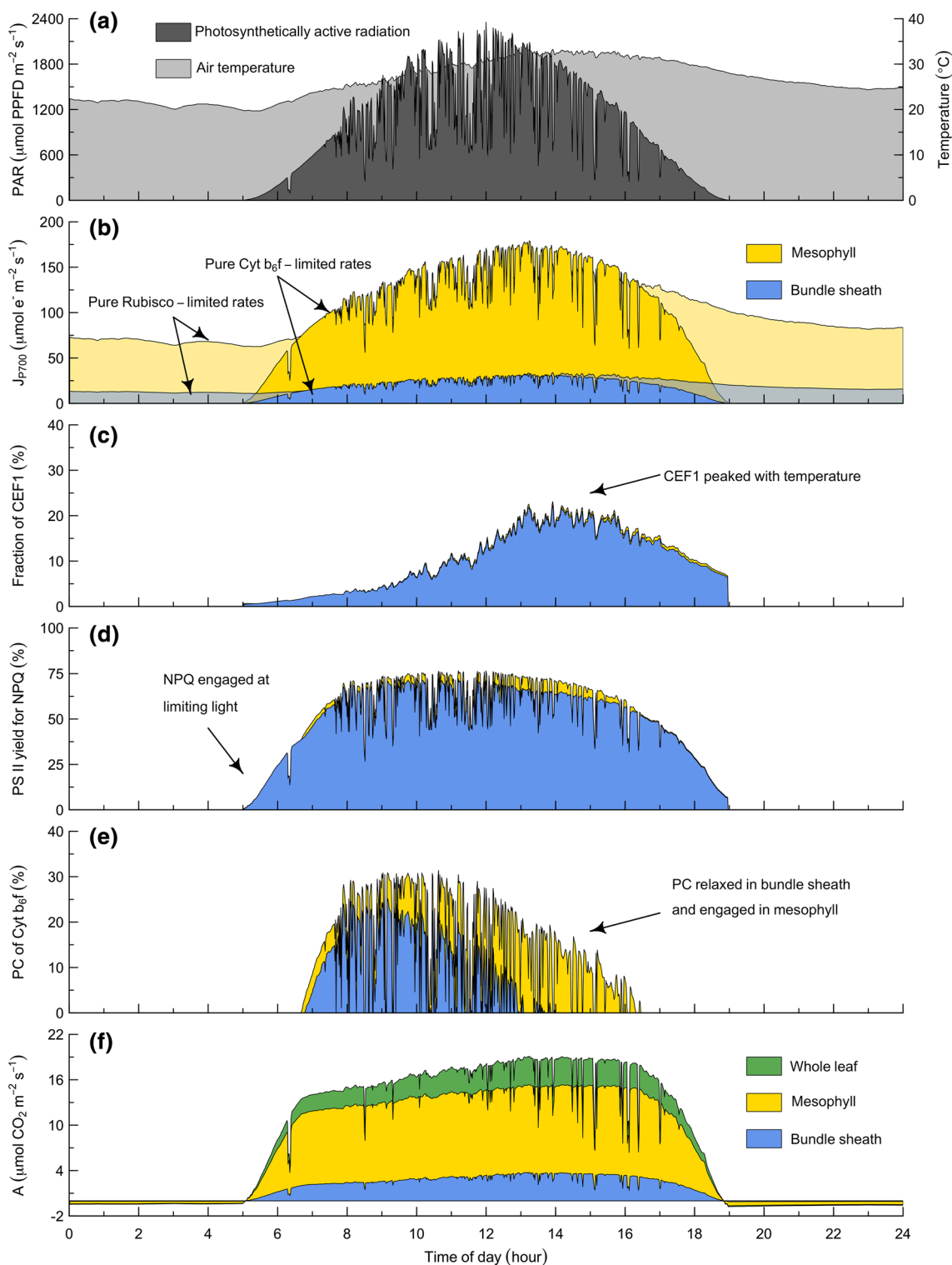


Fig. 7 Model simulation of the photosynthetic performance of *Flaveria chloraeifolia* (Type I C₃–C₄) over the diel cycle at the Diamond Y Spring Preserve. The photosynthesis model was parameterized with the fitted values of the physiological variables from the Texas site, and then driven with measurements of top-of-canopy irradiance and

air temperature from that site over one day in July. See text for details of methods and discussion of results. N.B., x-axes are the same for all panels. CEF1 cyclic electron flow around PS I, NPQ non-photochemical quenching of PS II, PC photosynthetic control of Cyt b_6f , PAR photosynthetically active radiation

change context, such understanding may have particularly important applications to conservation of rare, threatened, and endangered species (e.g., Pisanty et al. 2020) and engineering of the C₄ pathway into C₃ crops (e.g., Ermakova et al. 2020).

Conclusions

1. We have developed a quantitative model of C₃, C₃–C₄ intermediate, and C₄ photosynthesis that relates the factors limiting electron transport and carbon metabolism, the regulatory processes that coordinate these metabolic domains, and the overall responses to light, carbon dioxide, and temperature. The model describes the steady-state responses of leaf-level photosynthesis to these environmental factors within the ranges of conditions that leaves have acclimated to during growth.
2. This framework has three unique features. First, mechanistic expressions describe how the Cytochrome b₆f complex controls electron transport in mesophyll and bundle sheath chloroplasts. Second, the mesophyll and bundle sheath expressions are coupled in a way that represents how feedback regulation of Cyt b₆f coordinates electron transport and carbon metabolism. Third, the temperature sensitivity of Cyt b₆f is differentiated from that of the coupling between NADPH, Fd, and ATP production.
3. Using this framework, we have presented simulations demonstrating that the unique light dependence of the CO₂ compensation point in C₃–C₄ leaves can be explained by co-occurrence of light-saturation in the mesophyll and light-limitation in the bundle sheath. We have also presented inversions demonstrating that population-level variation in the CO₂ compensation point in a Type I C₃–C₄ species, *Flaveria chloraeifolia*, can be explained by variable allocation of photosynthetic capacity to the bundle sheath.
4. While there are substantial uncertainties about how the glycine shuttle works, this CO₂-concentrating mechanism is likely to provide advantages in the net CO₂ assimilation rate and resource-use efficiencies under some combinations of light, CO₂, and temperature, and disadvantages under others. C₃–C₄ intermediate plants may optimize pigment and protein distributions to maximize the benefits and minimize the costs of glycine shuttling under different environmental conditions.
5. Understanding this optimization quantitatively holds promise for explaining why the Type I C₃–C₄ pathway occupies such a key place in evolutionary history and yet remains so ecologically rare. It also holds promise for explaining the functional relationships between the

glycine, malate, and aspartate shuttles, and evaluating the hypothesis that the C₄ pathway originally evolved to smooth out energy supply and demand, rather than to concentrate CO₂.

Supplementary Information The online version contains supplementary material available at <https://doi.org/10.1007/s00442-021-05062-y>.

Acknowledgements This manuscript is to be published as part of a Special Issue honoring Russ Monson. We particularly appreciate Russ' contributions to understanding the physiology of the C₃–C₄ intermediates. R. Sage (University of Toronto, Canada) provided seeds to establish a research population of *F. chloraeifolia* at the Carnegie Institution. E. Slessarev (Lawrence Livermore National Laboratory) and C. Kouba (University of California Davis) assisted with the field studies. J. Karges and J. Wrinkle (The Nature Conservancy of Texas) granted permission to work at the Diamond Y Spring Preserve, and D. Roth (Energy, Minerals and Natural Resources Department of New Mexico) granted permission to work at the Blue Hole Ciénega. S. von Caemmerer (Australian National University, Australia) and W. Yamori (University of Tokyo, Japan) provided Cyt b₆f data for model evaluation. The manuscript was greatly improved by feedback from N. Smith (Texas Tech University) and two anonymous reviewers.

Author contribution statement JEJ and JAB conceived and designed the model. JEJ performed and analyzed the simulations. JEJ wrote the manuscript, with input from JAB and CBF.

Funding The authors acknowledge financial support from Stanford University (Bing-Mooney Fellowship in Environmental Science and Conservation), the National Science Foundation (Graduate Research Fellowship and Major Research Infrastructure Award 1040106), the Carnegie Institution for Science (Carnegie Science Venture Grant), and the National Aeronautics and Space Administration (New Investigator Program in Earth Science Award 20-NIP20-0242).

Availability of data and material The datasets analyzed in this study are available with the code, as described below.

Code availability The model described in this manuscript was implemented in MATLAB R2020b. The code is published under an MIT License, available on GitHub (<https://github.com/jenjohnson>), and archived on Zenodo (<https://doi.org/10.5281/zenodo.5577145>).

Declarations

Conflict of interest The authors declare no conflicts of interest.

Ethics approval Not applicable.

Consent to participate Not applicable.

Consent for publication Not applicable.

Open Access This article is licensed under a Creative Commons Attribution 4.0 International License, which permits use, sharing, adaptation, distribution and reproduction in any medium or format, as long as you give appropriate credit to the original author(s) and the source, provide a link to the Creative Commons licence, and indicate if changes

were made. The images or other third party material in this article are included in the article's Creative Commons licence, unless indicated otherwise in a credit line to the material. If material is not included in the article's Creative Commons licence and your intended use is not permitted by statutory regulation or exceeds the permitted use, you will need to obtain permission directly from the copyright holder. To view a copy of this licence, visit <http://creativecommons.org/licenses/by/4.0/>.

References

- Aldous SH, Weise SE, Sharkey TD, Waldera-Lupa DM, Stühler K, Mallman J, Groth G, Gowik U, Westhoff P, Arsova B (2014) Evolution of the phosphoenolpyruvate carboxylase protein kinase family in C₃ and C₄ *Flaveria* spp. *Plant Physiol* 165:1076–1091. <https://doi.org/10.1104/pp.114.240283>
- Apel P (1980) CO₂ compensation concentration and its O₂ dependence in *Moricandia spinosa* and *Moricandia moricandoides* (Cruciferae). *Biochem Physiol Pflanz* 175:386–388. [https://doi.org/10.1016/s0015-3796\(80\)80079-5](https://doi.org/10.1016/s0015-3796(80)80079-5)
- Baker NR, Harbinson J, Kramer DM (2007) Determining the limitations and regulation of photosynthetic energy transduction in leaves. *Plant Cell Environ* 30:1107–1125. <https://doi.org/10.1111/j.1365-3040.2007.01680.x>
- Bauwe H, Chollet R (1986) Kinetic properties of phosphoenolpyruvate carboxylase from C₃, C₄, and C₃-C₄ intermediate species of *Flaveria* (Asteraceae). *Plant Physiol* 82:695–699. <https://doi.org/10.1104/pp.82.3.695>
- Bellasio C (2017) A generalized stoichiometric model of C₃, C₂, C₂+C₄, and C₄ photosynthetic metabolism. *J Exp Bot* 68:269–282. <https://doi.org/10.1093/jxb/erw303>
- Bellasio C, Farquhar GD (2019) A leaf-level biochemical model simulating the introduction of C₂ and C₄ photosynthesis in C₃ rice: gains, losses and metabolite fluxes. *New Phytol* 223:150–166. <https://doi.org/10.1111/nph.15787>
- Bellasio C, Beerling DJ, Griffiths H (2016) Deriving C₄ photosynthetic parameters from combined gas exchange and chlorophyll fluorescence using an excel tool: theory and practice. *Plant, Cell Environ* 39:1164–1179. <https://doi.org/10.1111/pce.12626>
- Bernacchi CJ, Bagley JE, Serbin SP, Ruiz-Vera UM, Rosenthal DM (2013) Modelling C₃ photosynthesis from the chloroplast to the ecosystem. *Plant Cell Environ* 36:1641–1657. <https://doi.org/10.1111/pce.12118>
- Berry JA (1975) Adaptation of photosynthetic processes to stress. *Science* 188:644–650. <https://doi.org/10.1126/science.188.4188.644>
- Berry JA, Björkman O (1980) Photosynthetic response and adaptation to temperature in higher plants. *Annu Rev Plant Physiol* 31:491–543. <https://doi.org/10.1146/annurev.pp.31.060180.002423>
- Berry JA, Downton WJS (1982) Environmental regulation of photosynthesis. In: *Photosynthesis: development, carbon metabolism, and plant productivity*, vol 11. Academic Press, New York, pp 263–343. <https://doi.org/10.1016/b978-0-12-294302-7.50017-3>
- Berry JA, Farquhar GD (1978) The CO₂ concentrating function of C₄ photosynthesis: A biochemical model. In: Hall D, Coombs J, Goodwin T (eds) *Proceedings of the Fourth International Congress on Photosynthesis*, Reading, England. The Biochemical Society, London, p 119–131
- Berry JA, Raison JK (1981) Responses of macrophytes to temperature. In: Lange OL, Nobel PS, Osmond CB, Ziegler H (eds) *Physiological plant ecology I. Encyclopedia of plant physiology*, vol 12. Springer, Berlin, pp 277–338
- Björkman O, Gauthier E (1969) Carboxydismutase activity in plants with and without β-carboxylation photosynthesis. *Planta* 88:197–203. <https://doi.org/10.1007/bf00385062>
- Blackman FF (1905) Optima and limiting factors. *Ann Bot* 19:281–296. <https://doi.org/10.1093/oxfordjournals.aob.a089000>
- Bolton JK, Brown RH (1980) Photosynthesis of grass species differing in carbon dioxide fixation pathways: V. Response of *Panicum maximum*, *Panicum milioides*, and tall fescue (*Festuca arundinacea*) to nitrogen nutrition. *Plant Physiol* 66:97–100. <https://doi.org/10.1104/pp.66.1.97>
- Bowes G, Ogren WL, Hageman RH (1971) Phosphoglycolate production catalyzed by ribulose diphosphate carboxylase. *Biochem Biophys Res Commun* 45:716–722. [https://doi.org/10.1016/0006-291x\(71\)90475-x](https://doi.org/10.1016/0006-291x(71)90475-x)
- Brooks A, Farquhar GD (1985) Effect of temperature on the CO₂/O₂ specificity of ribulose-1,5-bisphosphate carboxylase oxygenase and the rate of respiration in the light: estimates from gas-exchange measurements on spinach. *Planta* 165:397–406. <https://doi.org/10.1007/bf00392238>
- Brown RH, Brown WV (1975) Photosynthetic characteristics of *Panicum milioides*, a species with reduced photorespiration. *Crop Sci* 15:681–685. <https://doi.org/10.2135/cropsci1975.0011183x001500050020x>
- Brown RH, Morgan JA (1980) Photosynthesis of grass species differing in carbon dioxide fixation pathways: VI. Differential effects of temperature and light intensity on photorespiration in C₃, C₄, and intermediate species. *Plant Physiol* 66:541–544. <https://doi.org/10.1104/pp.66.4.541>
- Brown RH, Simmons RE (1979) Photosynthesis of grass species differing in CO₂ fixation pathways. I. Water-use efficiency. *Crop Sci* 19:375–379. <https://doi.org/10.2135/cropsci1979.0011183x00183x001900030025x>
- Calvin M, Benson A (1948) The path of carbon in photosynthesis. *Science* 107:476–480. <https://doi.org/10.1126/science.107.2784.476>
- Chapman K, Berry JA, Hatch MD (1980) Photosynthetic metabolism in bundle sheath cells of the C₄ species *Zea mays*: sources of ATP and NADPH and the contribution of photosystem II. *Arch Biochem Biophys* 202:330–341. [https://doi.org/10.1016/0003-9861\(80\)90435-x](https://doi.org/10.1016/0003-9861(80)90435-x)
- Chastain CJ, Chollet R (1989) Interspecific variation in assimilation of ¹⁴CO₂ into C₄ acids by leaves of C₃, C₄, and C₃-C₄ intermediate *Flaveria* species near the CO₂ compensation concentration. *Planta* 179:81–88. <https://doi.org/10.1007/bf00395774>
- Cheng S-H, Moore BD, Wu J, Edwards GE, Ku MSB (1989) Photosynthetic plasticity in *Flaveria brownii*: growth irradiance and the expression of C₄ photosynthesis. *Plant Physiol* 89:1129–1135. <https://doi.org/10.1104/pp.89.4.1129>
- Chollet R, Vidal J, O'Leary M (1996) Phosphoenolpyruvate carboxylase: a ubiquitous, highly regulated enzyme in plants. *Annu Rev Plant Phys* 47:273–298. <https://doi.org/10.1146/annrev.arplant.47.1.273>
- Christin P-A, Osborne CP (2014) The evolutionary ecology of C₄ plants. *New Phytol* 204:765–781. <https://doi.org/10.1111/nph.13033>
- Christin P-A, Osborne CP, Sage RF, Arakaki M, Edwards E (2011) C₄ eudicots are not younger than C₄ monocots. *J Exp Bot* 62:3171–3181. <https://doi.org/10.1093/jxb/err041>
- Collatz GJ, Ball JT, Grivet C, Berry JA (1991) Physiological and environmental regulation of stomatal conductance, photosynthesis and transpiration: a model that includes a laminar boundary layer. *Ag Forest Meteorol* 54:107–136. [https://doi.org/10.1016/0168-1923\(91\)90002-8](https://doi.org/10.1016/0168-1923(91)90002-8)
- Collatz GJ, Berry JA, Clark J (1998) Effects of climate and atmospheric CO₂ partial pressure on the global distribution of C₄ grasses: present, past, and future. *Oecologia* 114:441–454. <https://doi.org/10.1007/s004420050468>
- Collatz GJ, Ribas-Carbó M, Berry JA (1992) Coupled photosynthesis-stomatal conductance model for leaves of C₄ plants. *Aust J Plant Physiol* 19:519–538. <https://doi.org/10.1071/pp9920519>

- Cornic G, Baker NR (2012) Electron transport in leaves: a physiological perspective. In: Eaton-Rye JJ, Tripathy BC, Sharkey TD (eds) Photosynthesis: plastid biology, energy conversion and carbon assimilation. Springer, New York, pp 591–606
- Čatský J, Tichá I (1979) CO₂ compensation concentration in bean leaves: effect of photon flux density and leaf age. Biol Plant 21:361–364. <https://doi.org/10.1007/bf02878234>
- Dai ZY, Ku M, Edwards GE (1996) Oxygen sensitivity of photosynthesis and photorespiration in different photosynthetic types in the genus *Flaveria*. Planta 198:563–571. <https://doi.org/10.1007/bf00262643>
- Demmig-Adams B, Garab G, Adams W III, Govindjee U (2014) Non-photochemical quenching and energy dissipation in plants, algae, and cyanobacteria. Advances in photosynthesis and respiration, vol 40. Springer, New York
- Duyvens LNM, Amesz J, Kamp BM (1961) Two photochemical systems in photosynthesis. Nature 190:510–511. <https://doi.org/10.1038/190510a0>
- Edwards GE, Ku MS (1987) Biochemistry of C₃–C₄ intermediates. In: Stumpf PK, Conn EE (eds) The biochemistry of plants. Academic Press, London, pp 275–325
- Ehleringer JR (1978) Implications of quantum yield differences on the distributions of C₃ and C₄ grasses. Oecologia 31:255–267. <https://doi.org/10.1007/bf00346246>
- Ehleringer J, Björkman O (1977) Quantum yields for CO₂ uptake in C₃ and C₄ plants: dependence on temperature, CO₂, and O₂ concentration. Plant Physiol 59:86–90. <https://doi.org/10.1104/pp.59.1.86>
- Ehleringer JR, Monson RK (1993) Evolutionary and ecological aspects of photosynthetic pathway variation. Ann Rev Ecol Syst 24:411–439. <https://doi.org/10.1146/annurev.es.24.110193.002211>
- Ehleringer J, Pearcy RW (1983) Variation in quantum yield for CO₂ uptake among C₃ and C₄ plants. Plant Physiol 73:555–559. <https://doi.org/10.1104/pp.73.3.555>
- Ehleringer JR, Cerling TE, Helliker BR (1997) C₄ photosynthesis, atmospheric CO₂ and climate. Oecologia 112:285–299. <https://doi.org/10.1007/s004420050311>
- Emerson R (1929) Photosynthesis as a function of light intensity and of temperature with different concentrations of chlorophyll. J Gen Physiology 12:623–639. <https://doi.org/10.1085/jgp.12.5.623>
- Engelmann S, Blasing OE, Gowik U, Svensson P, Westhoff P (2003) Molecular evolution of C₄ phosphoenolpyruvate carboxylase in the genus *Flaveria* – a gradual increase from C₃ to C₄ characteristics. Planta 217:717–725. <https://doi.org/10.1007/s00425-003-1045-0>
- Ermakova M, Danila FR, Furbank RT, von Caemmerer S (2020) On the road to C₄ rice: advances and perspectives. Plant J 101:940–950. <https://doi.org/10.1111/tpj.14562>
- Farquhar GD, von Caemmerer S (1981) Electron transport limitations on the CO₂ assimilation rate of leaves: a model and some observations in *Phaseolus vulgaris*. In: Akoyunoglou G (eds) Proceedings of the Fifth International Congress on Photosynthesis. Philadelphia, p 163–175
- Farquhar GD, von Caemmerer S, Berry JA (1980a) A biochemical model of photosynthetic CO₂ assimilation in leaves of C₃ species. Planta 149:78–90. <https://doi.org/10.1007/bf00386231>
- Farquhar GD, Firth PM, Wetselaar R, Weir B (1980b) On the gaseous exchange of ammonia between leaves and the environment—determination of the ammonia compensation point. Plant Physiol 66:710–714. <https://doi.org/10.1104/pp.66.4.710>
- Field CB (1983) Allocating leaf nitrogen for the maximization of carbon gain: leaf age as a control on the allocation program. Oecologia 56:341–347. <https://doi.org/10.1007/bf00379710>
- Field CB, Mooney HA (1986) The photosynthesis-nitrogen relationship in wild plants. In: Givnish TJ (ed) On the economy of plant form and function: Proceedings of the Sixth Maria Moors Cabot Symposium. Cambridge University Press, Cambridge, UK, p 22–55
- Field CB, Merino J, Mooney HA (1983) Compromises between water-use efficiency and nitrogen-use efficiency in five species of California evergreens. Oecologia 60:384–389. <https://doi.org/10.1007/bf00376856>
- Finazzi G, Minagawa J, Johnson GN (2016) The cytochrome b₆f complex: a regulatory hub controlling electron flow and the dynamics of photosynthesis? In: Cramer WA, Kallas T (eds) Cytochrome complexes: evolution, structures, energy transduction, and signaling. Springer, Dordrecht, pp 437–452
- Fladung M, Hesselbach J (1989) Effect of varying environments on photosynthetic parameters of C₃, C₃–C₄ and C₄ species of *Panicum*. Oecologia 79:168–173. <https://doi.org/10.1007/bf00388473>
- Foyer C, Furbank R, Harbinson J, Horton P (1990) The mechanisms contributing to photosynthetic control of electron transport by carbon assimilation in leaves. Photosynth Res 25:83–100. <https://doi.org/10.1007/bf00035457>
- Foyer CH, Neukermans J, Queval G, Noctor G, Harbinson J (2012) Photosynthetic control of electron transport and the regulation of gene expression. J Exp Bot 63:1637–1661. <https://doi.org/10.1093/jxb/ers013>
- Furbank RT, Taylor WC (1995) Regulation of photosynthesis in C₃ and C₄ plants: a molecular approach. Plant Cell 7:797–807. <https://doi.org/10.1105/tpc.7.7.797>
- Furbank RT, Jenkins CLD, Hatch MD (1990) C₄ photosynthesis: quantum requirement, C₄ and overcycling and Q-cycle involvement. Funct Plant Biol 17:1–7. <https://doi.org/10.1071/pp9900001>
- Genty B, Harbinson J (1996) Regulation of light utilization for photosynthetic electron transport. In: Baker NR (ed) Photosynthesis and the environment. Kluwer Academic Publishers, Amsterdam, pp 67–99
- Gould SJ, Lewontin RC (1979) The spandrels of San Marco and the Panglossian paradigm: a critique of the adaptationist programme. Proc R Soc Lond B Biol Sci 205:581–598. <https://doi.org/10.1098/rspb.1979.0086>
- Harbinson J, Genty B, Foyer CH (1990) Relationship between photosynthetic electron transport and stromal enzyme activity in pea leaves: toward an understanding of the nature of photosynthetic control. Plant Physiol 94:545–553. <https://doi.org/10.1104/pp.94.2.545>
- Hatch MD (1987) C₄ photosynthesis: a unique blend of modified biochemistry, anatomy and ultrastructure. Biochim Biophys Acta 895:81–106. [https://doi.org/10.1016/s0304-4173\(87\)80009-5](https://doi.org/10.1016/s0304-4173(87)80009-5)
- Hatch MD, Kagawa T, Craig S (1975) Subdivision of C₄-pathway species based on differing C₄ acid decarboxylating systems and ultrastructural features. Aust J Plant Physiol 2:111–128. <https://doi.org/10.1071/pp9750111>
- Hattersley PW, Wong SC, Perry S, Roksandic Z (1986) Comparative ultrastructure and gas exchange characteristics of the C₃–C₄ intermediate *Neurachne minor* ST Blake (Poaceae). Plant Cell Environ 9:217–233. <https://doi.org/10.1111/1365-3040.ep11611656>
- Heber U, Neimanis S, Dietz KJ, Viil J (1986) Assimilatory power as a driving force in photosynthesis. Biochim Biophys Acta 852:144–155. [https://doi.org/10.1016/0005-2728\(86\)90067-8](https://doi.org/10.1016/0005-2728(86)90067-8)
- Heckmann D, Schulze S, Denton A, Gowik U, Westhoff P, Weber APM (2013) Predicting C₄ photosynthesis evolution: modular, individually adaptive steps on a Mount Fuji fitness landscape. Cell 153:1579–1588. <https://doi.org/10.1016/j.cell.2013.04.058>
- Henning JC, Brown RH (1986) Effects of irradiance and temperature on photosynthesis in C₃, C₄, and C₃/C₄ *Panicum* species. Photosynth Res 10:101–112. <https://doi.org/10.1007/bf00024189>

- Holaday AS, Chollet R (1984) Photosynthetic/photorespiratory characteristics of C₃–C₄ intermediate species. *Photosynth Res* 5:307–323. <https://doi.org/10.1007/bf00034976>
- Holaday AS, Harrison AT, Chollet R (1982) Photosynthetic/photorespiratory CO₂ exchange characteristics of the C₃–C₄ intermediate species, *Moricandia arvensis*. *Plant Sci Lett* 27:181–189. [https://doi.org/10.1016/0304-4211\(82\)90147-x](https://doi.org/10.1016/0304-4211(82)90147-x)
- Holaday AS, Lee KW, Chollet R (1984) C₃–C₄ intermediate species in the genus *Flaveria*: leaf anatomy, ultrastructure, and the effect of O₂ on the CO₂ compensation concentration. *Planta* 160:25–32. <https://doi.org/10.1007/bf00392462>
- Hunt S, Smith AM, Woolhouse HW (1987) Evidence for a light-dependent system for reassimilation of photorespiratory CO₂, which does not include a C₄ cycle, in the C₃–C₄ intermediate species *Moricandia arvensis*. *Planta* 171:227–234. <https://doi.org/10.1007/bf00391098>
- Huxman TE, Monson RK (2003) Stomatal responses of C₃, C₃–C₄ and C₄ *Flaveria* species to light and intercellular CO₂ concentration: implications for the evolution of stomatal behaviour. *Plant Cell Environ* 26:313–322. <https://doi.org/10.1046/j.1365-3040.2003.00964.x>
- Hylton CM, Rawsthorne S, Smith AM, Jones DA, Woolhouse HW (1988) Glycine decarboxylase is confined to the bundle-sheath cells of leaves of C₃–C₄ intermediate species. *Planta* 175:452–459. <https://doi.org/10.1007/bf00393064>
- Ivanov AG, Velitchkova MY, Allakhverdiev SI, Huner NPA (2017) Heat stress-induced effects of photosystem I: an overview of structural and functional responses. *Photosynth Res* 133:17–30. <https://doi.org/10.1007/s11120-017-0383-x>
- Johnson JE, Berry JA (2013) The influence of leaf-atmosphere NH₃(g) exchange on the isotopic composition of nitrogen in plants and the atmosphere. *Plant Cell Environ* 36:1783–1801. <https://doi.org/10.1111/pce.12087>
- Johnson JE, Berry JA (2021) The role of cytochrome b₆f in the control of steady-state photosynthesis: a conceptual and quantitative model. *Photosynth Res* 148:101–136. <https://doi.org/10.1007/s11120-021-00840-4>
- Kallas T (2012) Cytochrome b₆f complex at the heart of energy transduction and redox signaling. In: Eaton-Rye JJ, Tripathy BC, Sharkey TD (eds) Photosynthesis: plastid biology, energy conversion and carbon assimilation. Springer, New York, pp 501–560
- Keck RW, Ogren WL (1976) Differential oxygen response of photosynthesis in soybean and *Panicum milioides*. *Plant Physiol* 58:552–555. <https://doi.org/10.1104/pp.58.4.552>
- Keerberg O, Pärnik T, Ivanova H, Bassüner B, Bauwe H (2014) C₂ photosynthesis generates about 3-fold elevated leaf CO₂ levels in the C₃–C₄ intermediate species *Flaveria pubescens*. *J Exp Bot* 65:3649–3656. <https://doi.org/10.1093/jxb/eru239>
- Kennedy RA, Laetsch WM (1974) Plant species intermediate for C₃, C₄ photosynthesis. *Science* 184:1087–1089. <https://doi.org/10.1126/science.184.4141.1087>
- Khoshravesh R, Stinson CR, Stata M, Busch FA, Sage RA (2016) C₃–C₄ intermediacy in grasses: organelle enrichment and distribution, glycine decarboxylase expression, and the rise of C₂ photosynthesis. *J Exp Bot* 67:3065–3078. <https://doi.org/10.1093/jxb/erw150>
- Kocacinar F, McKown AD, Sage TL, Sage RF (2008) Photosynthetic pathway influences xylem structure and function in *Flaveria* (Asteraceae). *Plant Cell Environ* 31:1363–1376. <https://doi.org/10.1111/j.1365-3040.2008.01847.x>
- Kopriva S, Chu C, Bauwe H (1996) Molecular phylogeny of *Flaveria* as deduced from the analysis of nucleotide sequences encoding the H-protein of the glycine cleavage system. *Plant Cell Environ* 19:1028–1036. <https://doi.org/10.1111/j.1365-3040.1996.tb00209.x>
- Kortschak HP, Hartt CE, Burr GO (1965) Carbon dioxide fixation in sugarcane leaves. *Plant Physiol* 40:209–213. <https://doi.org/10.1104/pp.40.2.209>
- Krall JP, Edwards GE, Ku M (1991) Quantum yield of photosystem II and efficiency of CO₂ fixation in *Flaveria* (Asteraceae) species under varying light and CO₂. *Aust J Plant Physiol* 18:369–383. <https://doi.org/10.1071/pp9910369>
- Ku M, Wu JR, Dai ZY, Scott RA, Chu C, Edwards GE (1991) Photosynthetic and photorespiratory characteristics of *Flaveria* species. *Plant Physiol* 96:518–528. <https://doi.org/10.1104/pp.96.2.518>
- Laing WA, Ogren WL, Hageman RH (1974) Regulation of soybean net photosynthetic CO₂ fixation by the interaction of CO₂, O₂, and ribulose 1,5-diphosphate carboxylase. *Plant Physiol* 54:678–685. <https://doi.org/10.1104/pp.54.5.678>
- Laisk A, Edwards GE (2000) A mathematical model of C₄ photosynthesis: The mechanism of concentrating CO₂ in NADP-malic enzyme type species. *Photosynth Res* 66:199–224. <https://doi.org/10.1023/a:1010695402963>
- Laisk A, Eichelmann H, Oja V (2009) Leaf C₃ photosynthesis in silico: integrated carbon/nitrogen metabolism. In: Laisk A, Nedbal L, Govindjee U (eds) Photosynthesis in silico: understanding complexity from molecules to ecosystems, vol 29. Springer, Dordrecht, pp 295–322
- Leegood RC, von Caemmerer S (1994) Regulation of photosynthetic carbon assimilation in leaves of C₃–C₄ intermediate species of *Moricandia* and *Flaveria*. *Planta* 192:232–238. <https://doi.org/10.1007/bf00194457>
- Leegood RC, Walker RP (1999) Regulation of the C₄ pathway. In: Sage RF, Monson RK (eds) C₄ plant biology. Elsevier, New York, pp 89–131
- Leonardos ED, Grodzinski B (2000) Photosynthesis, immediate export and carbon partitioning in source leaves of C₃, C₃–C₄ intermediate, and C₄ *Panicum* and *Flaveria* species at ambient and elevated CO₂ levels. *Plant Cell Environ* 23:839–851. <https://doi.org/10.1046/j.1365-3040.2000.00604.x>
- Leonardos ED, Grodzinski B (2003) Export patterns of ¹⁴C-assimilates from source leaves of C₃, C₃–C₄ intermediate, and C₄ *Panicum* and *Flaveria* species during light and dark periods. *Can J Bot* 81:464–476. <https://doi.org/10.1139/b03-041>
- Lundgren MR (2020) C₂ photosynthesis: a promising route towards crop improvement? *New Phytol* 228:1734–1740. <https://doi.org/10.1111/nph.16494>
- Lundgren MR, Christin P-A (2017) Despite phylogenetic effects, C₃–C₄ lineages bridge the ecological gap to C₄ photosynthesis. *J Exp Bot* 68:241–254. <https://doi.org/10.1093/jxb/erw451>
- Lundgren MR, Christin P-A, Escobar EG, Ripley BS, Besnard G, Long CM, Hattersley PW, Ellis RP, Osborne LRC (2016) Evolutionary implications of C₃–C₄ intermediates in the grass *Alloteropsis semialata*. *Plant Cell Environ* 39:1874–1885. <https://doi.org/10.1111/pce.12665>
- Lyu M-JA, Gowik U, Kelly S, Covshoff S, Hibberd JM, Sage RF, Ludwig M, Wong GK-S, Westhoff P, Zhu X-G (2021) The coordination of major events in C₄ photosynthesis evolution in the genus *Flaveria*. *Sci Rep* 11:15618. <https://doi.org/10.1038/s41598-021-93381-8>
- Mallmann J, Heckmann D, Bräutigam A, Lercher MJ, Weber APM, Westhoff P, Gowik U (2014) The role of photorespiration during the evolution of C₄ photosynthesis in the genus *Flaveria*. *Elife* 3:e02478. <https://doi.org/10.7554/elife.02478>
- Malone LA, Proctor MS, Hitchcock A, Hunter CN, Johnson MP (2021) Cytochrome b₆f—orchestrator of photosynthetic electron transfer. *Biochim Biophys Acta* 1862:148380. <https://doi.org/10.1016/j.bbabiobio.2021.148380>

- Maynard Smith J, Price GR (1973) The logic of animal conflict. *Nature* 246:15–18. <https://doi.org/10.1038/246015a0>
- McKown AD, Dengler NG (2007) Key innovations in the evolution of Kranz anatomy and C₄ vein pattern in *Flaveria* (Asteraceae). *Am J Bot* 94:382–399. <https://doi.org/10.3732/ajb.94.3.382>
- McKown AD, Moncalvo JM, Dengler NG (2005) Phylogeny of *Flaveria* (Asteraceae) and inference of C₄ photosynthesis evolution. *Am J Bot* 92:1911–1928. <https://doi.org/10.3732/ajb.92.11.1911>
- Monson RK (1989a) On the evolutionary pathways resulting in C₄ photosynthesis and crassulacean acid metabolism (CAM). *Adv Ecol Res* 19:57–110. [https://doi.org/10.1016/S0065-2504\(08\)60157-9](https://doi.org/10.1016/S0065-2504(08)60157-9)
- Monson RK (1989b) The relative contributions of reduced photorespiration, and improved water-use and nitrogen-use efficiencies, to the advantages of C₃–C₄ intermediate photosynthesis in *Flaveria*. *Oecologia* 80:215–221. <https://doi.org/10.1007/bf00380154>
- Monson RK (2003) Gene duplication, neofunctionalization, and the evolution of C₄ photosynthesis. *Int J Plant Sci* 164:S43–S54. <https://doi.org/10.1086/368400>
- Monson RK, Edwards GE, Ku M (1984) C₃–C₄ intermediate photosynthesis in plants. *Bioscience* 34:563–574. <https://doi.org/10.2307/1309599>
- Monson RK, Moore BD, Ku M, Edwards GE (1986) Cofunction of C₃- and C₄-photosynthetic pathways in C₃, C₄, and C₃–C₄ intermediate *Flaveria* species. *Planta* 168:493–502. <https://doi.org/10.1007/bf00392268>
- Monson RK, Rawsthorne S (2000) CO₂ assimilation in C₃–C₄ intermediate plants. In: *Photosynthesis: physiology and metabolism*. Kluwer Academic Publishers, Amsterdam, pp 533–550
- Moore BD, Franceschi VR, Cheng S-H, Wu J, Ku MSB (1987a) Photosynthetic characteristics of the C₃–C₄ intermediate *Parthenium hysterophorus*. *Plant Physiol* 85:978–983. <https://doi.org/10.1104/pp.85.4.978>
- Moore BD, Ku M, Edwards GE (1987b) C₄ photosynthesis and light-dependent accumulation of inorganic carbon in leaves of C₃–C₄ and C₄ *Flaveria* species. *Aust J Plant Physiol* 14:657–668. <https://doi.org/10.1071/pp9870657>
- Morales A, Yin X, Harbinson J, Driever SM, Molenaar J, Kramer DM, Struik PC (2018) In silico analysis of the regulation of the photosynthetic electron transport chain in C₃ plants. *Plant Physiol* 176:1247–1261. <https://doi.org/10.1104/pp.17.00779>
- Morgan JA, Brown RH (1980) Photosynthesis in grass species differing in carbon dioxide fixation pathways: III. Oxygen response and enzyme activities of species in the Laxa group of *Panicum*. *Plant Physiol* 65:156–159. <https://doi.org/10.1104/pp.65.1.156>
- Ochoterena H, Flores-Olvera H, Gómez-Hinostrosa C, Moore MJ (2020) Gypsum and plant species: a marvel of Cuatro Ciénegas and the Chihuahuan desert. In: Mandujano M, Pisanty I, Eguiarte L (eds) *Plant diversity and ecology in the Chihuahuan desert. Cuatro Ciénegas basin: an endangered hyperdiverse oasis*. Springer, Cham, pp 129–166
- Ogren WL, Bowes G (1971) Ribulose diphosphate carboxylase regulates soybean photorespiration. *Nat New Biol* 230:159–160. <https://doi.org/10.1038/newbio230159a0>
- Osborne CP, Beerling DJ (2006) Nature's green revolution: the remarkable evolutionary rise of C₄ plants. *Philos Trans R Soc Lond B Biol Sci* 361:173–194. <https://doi.org/10.1098/rstb.2005.1737>
- Osborne CP, Sack L (2012) Evolution of C₄ plants: a new hypothesis for an interaction of CO₂ and water relations mediated by plant hydraulics. *Philos Trans R Soc Lond B Biol Sci* 367:583–600. <https://doi.org/10.1098/rstb.2011.0261>
- Pearcy RW, Ehleringer JR (1984) Comparative ecophysiology of C₃ and C₄ plants. *Plant Cell Environ* 7:1–13. <https://doi.org/10.1111/j.1365-3040.1984.tb01194.x>
- Peisker M (1979) Conditions for low, and oxygen-independent, CO₂ compensation concentrations in C₄ plants as derived from a simple model. *Photosynthetica* 13:198–207
- Peisker M (1984) Modellvorstellungen zur kohlenstoff-isotopenidisierung bei der photosynthese von C₃- und C₄-pflanzen. *Kulturpflanze* 32:35–65. <https://doi.org/10.1007/bf02098683>
- Peisker M (1986) Models of carbon metabolism in C₃–C₄ intermediate plants as applied to the evolution of C₄ photosynthesis. *Plant Cell Environ* 9:627–635. <https://doi.org/10.1111/j.1365-3040.1986.tb01620.x>
- Peisker M, Bauwe H (1984) modeling carbon metabolism in C₃–C₄ intermediate species. 1. CO₂ compensation concentration and its O₂ dependence. *Photosynthetica* 18:9–19
- Peisker M, Henderson SA (1992) Carbon: terrestrial C₄ plants. *Plant Cell Environ* 15:987–1004. <https://doi.org/10.1111/j.1365-3040.1992.tb01651.x>
- Peralta-García C, Sanchez-Coronado ME, Orozco-Segovia A, Orozco-Segovia S, Pisanty-Baruch I (2016) Germination of four riparian species in a disturbed semi-arid ecosystem. *S Afr J Bot* 106:110–118. <https://doi.org/10.1016/j.sajb.2016.06.006>
- Peralta-García C, Pisanty I, Orozco-Segovia A, Sánchez-Coronado ME, Rodríguez-Sánchez M (2020) Germination of riparian species in natural and experimental conditions. In: Mandujano M, Pisanty I, Eguiarte L (eds) *Plant diversity and ecology in the Chihuahuan desert. Cuatro Ciénegas basin: an endangered hyperdiverse oasis*. Springer, Cham, pp 309–320
- Pfündel E, Pfeffer M (1997) Modification of photosystem I light harvesting of bundle-sheath chloroplasts occurred during the evolution of NADP-malic enzyme C₄ photosynthesis. *Plant Physiol* 114:145–152. <https://doi.org/10.1104/pp.114.1.145>
- Pinto H, Tissue DT, Ghannoum O (2011) *Panicum milioides* (C₃–C₄) does not have improved water or nitrogen economies relative to C₃ and C₄ congeners exposed to industrial-age climate change. *J Exp Bot* 62:3223–3234. <https://doi.org/10.1093/jxb/err005>
- Pinto H, Sharwood RE, Tissue DT, Ghannoum O (2014) Photosynthesis of C₃, C₃–C₄, and C₄ grasses at glacial CO₂. *J Exp Bot* 65:3669–3681. <https://doi.org/10.1093/jxb/eru155>
- Pisanty I, Rodríguez-Sánchez M, Orozco PT, Granados-Hernández LA, Escobar S, Mandujano MC (2020) Disturbance and the formation and colonization of new habitats in a hydrological system in the Cuatro Ciénegas basin. In: Mandujano M, Pisanty I, Eguiarte L (eds) *Plant diversity and ecology in the Chihuahuan desert. Cuatro Ciénegas basin: an endangered hyperdiverse oasis*. Springer, Cham, pp 265–282
- Powell AM (1978) Systematics of *Flaveria* (Flaveriinae Asteraceae). *Ann Mo Bot Gard* 65:590–636. <https://doi.org/10.2307/2398862>
- Quebedeaux B, Chollet R (1977) Comparative growth analyses of panicum species with differing rates of photorespiration. *Plant Physiol* 59:42–44. <https://doi.org/10.1104/pp.59.1.42>
- Rabinowitch E (1951) Photosynthesis and related processes, part 1, vol 2. Interscience Publishers, New York, pp 600–1208
- Rajendrudu G, Prasad JS, Das VR (1986) C₃–C₄ intermediate species in *Alternanthera* (Amaranthaceae) leaf anatomy, CO₂ compensation point, net CO₂ exchange and activities of photosynthetic enzymes. *Plant Physiol* 80:409–414. <https://doi.org/10.1104/pp.80.2.409>
- Rawsthorne S (1992) C₃–C₄ intermediate photosynthesis: linking physiology to gene expression. *Plant J* 2:267–274. <https://doi.org/10.1111/j.1365-313x.1992.00267.x>
- Rawsthorne S, Hylton CM (1991) The relationship between the post-illumination CO₂ burst and glycine metabolism in leaves of C₃ and C₃–C₄ intermediate species of *Moricandia*. *Planta* 186:122–126. <https://doi.org/10.1007/bf00201507>
- Rawsthorne S, von Caemmerer S, Brooks A, Leegood RC (1992) Metabolic interactions in leaves of C₃–C₄ intermediate plants. In:

- Tobin AK (ed) Plant organelles compartmentation of metabolism in photosynthetic cells. Cambridge University Press, Cambridge, pp 113–139
- Rawsthorne S, Hylton CM, Smith AM, Woolhouse HW (1988a) Photorespiratory metabolism and immunogold localization of photorespiratory enzymes in leaves of C_3 and C_3-C_4 intermediate species of *Moricandia*. *Planta* 173:298–308. <https://doi.org/10.1007/bf00401016>
- Rawsthorne S, Hylton CM, Smith AM, Woolhouse HW (1988b) Distribution of photorespiratory enzymes between bundle-sheath and mesophyll cells in leaves of the C_3-C_4 intermediate species *Moricandia arvensis* (L) DC. *Planta* 176:527–532. <https://doi.org/10.1007/bf00397660>
- Reed JE, Chollet R (1985) Immunofluorescent localization of phosphoenolpyruvate carboxylase and ribulose 1,5-bisphosphate carboxylase/oxygenase proteins in leaves of C_3 , C_4 and C_3-C_4 intermediate *Flaveria* species. *Planta* 165:439–445. <https://doi.org/10.1007/bf00398088>
- Rodríguez-Sánchez M, Pisanty I, Mandujano MC, Flores-Olvera H, Almaguer AK (2020) An unlikely movable feast in a desert hydrological system: why do life cycles matter. In: Mandujano M, Pisanty I, Eguiarte L (eds) Plant diversity and ecology in the Chihuahuan desert. Cuatro Ciénegas basin: an endangered hyperdiverse oasis. Springer, Cham, pp 283–296
- Sage RF, Khoshravesh R, Sage TL (2014) From proto-Kranz to C_4 Kranz: building the bridge to C_4 photosynthesis. *J Exp Bot* 65:3341–3356. <https://doi.org/10.1093/jxb/eru180/-dc1>
- Sage RF, Sage TL, Kocacinar F (2012) Photorespiration and the evolution of C_4 photosynthesis. *Annu Rev Plant Biol* 63:19–47. <https://doi.org/10.1146/annurev-arplant-042811-105511>
- Sage RF, Monson RK, Ehleringer JR, Adachi S, Pearcey RW (2018) Some like it hot: the physiological ecology of C_4 plant evolution. *Oecologia* 187:941–966. <https://doi.org/10.1007/s00442-018-4191-6>
- Sarewicz M, Pintscher S, Pietras R, Borek A, Bujnowicz L, Hanke G, Cramer WA, Finazzi G, Osyczka O (2021) Catalytic reactions and energy conservation in the cytochrome bc₁ and b₆f complexes of energy-transducing membranes. *Chem Rev* 121:2020–2108. <https://doi.org/10.1021/acs.chemrev.0c00712>
- Sarojini G, Oliver DJ (1983) Extraction and partial characterization of the glycine decarboxylase multienzyme complex from pea leaf mitochondria. *Plant Physiol* 72:194–199. <https://doi.org/10.1104/pp.72.1.194>
- Schlüter U, Weber APM (2020) Regulation and evolution of C_4 photosynthesis. *Annu Rev Plant Biol* 71:183–215. <https://doi.org/10.1146/annurev-arplant-042916-040915>
- Schlüter U, Brautigam A, Gowik U, Melzer M, Christin P-A, Kurz S, Mettler-Altmann T, Weber APM (2017) Photosynthesis in C_3-C_4 intermediate *Moricandia* species. *J Exp Bot* 68:191–206. <https://doi.org/10.1093/jxb/erw391>
- Schöttler MA, Tóth SZ (2014) Photosynthetic complex stoichiometry dynamics in higher plants: environmental acclimation and photosynthetic flux control. *Front Plant Sci* 5:1–15. <https://doi.org/10.3389/fpls.2014.00188>
- Schulze S, Mallmann J, Burscheidt J, Koczor M, Streubel M, Bauwe H, Gowik U, Westhoff P (2013) Evolution of C_4 photosynthesis in the genus *Flaveria*: establishment of a photorespiratory CO₂ pump. *The Plant Cell Online* 25:2522–2535. <https://doi.org/10.1105/tpc.113.114520>
- Schuster WS, Monson RK (1990) An examination of the advantages of C_3-C_4 intermediate photosynthesis in warm environments. *Plant Cell Environ* 13:903–912. <https://doi.org/10.1111/j.1365-3040.1990.tb01980.x>
- Sellers PJ, Randall DA, Collatz GJ, Berry JA, Field CF, Dazlich DA, Zhang C, Collelo GD, Bounoua L (1996a) A revised land surface parameterization (SiB2) for atmospheric GCMS Part I: model formulation. *J Climate* 9:676–705. [https://doi.org/10.1175/1520-0442\(1996\)009%3c0676:arlspf%3e2.0.co;2](https://doi.org/10.1175/1520-0442(1996)009%3c0676:arlspf%3e2.0.co;2)
- Sellers PJ, Tucker CJ, Collatz GJ, Los SO, Justice CO, Dazlich DA, Randall DA (1996b) A revised land surface parameterization (SiB2) for atmospheric GCMs. Part II: the generation of global fields of terrestrial biophysical parameters from satellite data. *J Climate* 9:706–737. [https://doi.org/10.1175/1520-0442\(1996\)009%3c0706:arlspf%3e2.0.co;2](https://doi.org/10.1175/1520-0442(1996)009%3c0706:arlspf%3e2.0.co;2)
- Sharkey TD, Zhang R (2010) High temperature effects on electron and proton circuits of photosynthesis. *J Integr Plant Biol* 52:712–722. <https://doi.org/10.1111/j.1744-7909.2010.00975.x>
- Simkin AJ, López-Calcagno PE, Raines CA (2019) Feeding the world: improving photosynthetic efficiency for sustainable crop production. *J Exp Bot* 70:1119–1140. <https://doi.org/10.1093/jxb/ery445>
- Slack CR, Hatch MD (1967) Comparative studies on activity of carboxylases and other enzymes in relation to new pathway of photosynthetic carbon dioxide fixation in tropical grasses. *Biochem J* 103:660–665. <https://doi.org/10.1042/bj1030660>
- Sata M, Sage TL, Hoffman N, Covshoff S, Wong GK-S, Sage RF (2016) Mesophyll chloroplast investment in C_3 , C_4 and C_2 species of the genus *Flaveria*. *Plant Cell Physiol* 57:904–918. <https://doi.org/10.1093/pcp/pcw015>
- Sata M, Sage TL, Sage RF (2019) Mind the gap: the evolutionary engagement of the C_4 metabolic cycle in support of net carbon assimilation. *Curr Opin Plant Biol* 49:27–34. <https://doi.org/10.1016/j.pbi.2019.04.008>
- Stiehl HH, Witt HT (1969) Quantitative treatment of the function of plastoquinone in photosynthesis. *Zeitschrift Für Naturforschung B* 24:1588–1598. <https://doi.org/10.1515/znb-1969-1219>
- Still CJ, Berry JA, Collatz GJ, DeFries RS (2003) Global distribution of C_3 and C_4 vegetation: carbon cycle implications. *Global Biogeochem Cycles* 17:1006. <https://doi.org/10.1029/2001gb001807>
- Sundermann EM, Lercher MJ, Heckmann D (2021) Modeling photosynthetic resource allocation connects physiology with evolutionary environments. *Sci Rep* 11:15979. <https://doi.org/10.1038/s41598-021-94903-0>
- Tagawa K, Tsujimoto HY, Arnon DI (1963) Role of chloroplast ferredoxin in the energy conversion process of photosynthesis. *Proc National Acad Sci* 49:567–572. <https://doi.org/10.1073/pnas.49.4.567>
- Thornley JHM (1976) Mathematical models in plant physiology. Academic Press, London, pp 1–318
- Tikhonov AN (2018) The cytochrome b₆f complex: biophysical aspects of its functioning in chloroplasts. In: Harris JR, Boekema EJ (eds) Membrane protein complexes: structure and function. Springer, Singapore, pp 287–328
- Tikkanen M, Grieco M, Nurmi M, Rantala M, Suorsa M, Aro E-M (2012) Regulation of the photosynthetic apparatus under fluctuating growth light. *Phil Trans R Soc B Biol Sci* 367:3486–3493. <https://doi.org/10.1098/rstb.2012.0067>
- Tipple BJ, Pagani M (2007) The early origins of terrestrial C_4 photosynthesis. *Ann Rev Earth Planet Sci* 35:435–461. <https://doi.org/10.1146/annurev.earth.35.031306.140150>
- Tregunna EB, Krotkov G, Nelson CD (1966) Effect of oxygen on the rate of photorespiration in detached tobacco leaves. *Physiol Plantarum* 19:723–733. <https://doi.org/10.1111/j.1399-3054.1966.tb07057.x>
- Van Auken OW, Grunstra M, Brown SC (2007) Composition and structure of a West Texas salt marsh. *Madroño* 54:138–147. [https://doi.org/10.3120/0024-9637\(2007\)54%5b138:casoaw%5d2.0.co;2](https://doi.org/10.3120/0024-9637(2007)54%5b138:casoaw%5d2.0.co;2)
- van der Tol C, Berry JA, Campbell PKE, Rascher U (2014) Models of fluorescence and photosynthesis for interpreting measurements of solar-induced chlorophyll fluorescence. *J Geophys Res Biogeosci* 119:2312–2327. <https://doi.org/10.1002/2014jg002713>

- Vogan PJ, Sage RF (2011) Water-use efficiency and nitrogen-use efficiency of C₃–C₄ intermediate species of *Flaveria* Juss. (Asteraceae). *Plant Cell Environ* 34:1415–1430. <https://doi.org/10.1111/j.1365-3040.2011.02340.x>
- Vogan PJ, Frohlich MW, Sage RF (2007) The functional significance of C₃–C₄ intermediate traits in *Heliotropium* L. (Boraginaceae): gas exchange perspectives. *Plant Cell Environ* 30:1337–1345. <https://doi.org/10.1111/j.1365-3040.2007.01706.x>
- Vogan PJ, Sage RF (2012) Effects of low atmospheric CO₂ and elevated temperature during growth on the gas exchange responses of C₃, C₃–C₄ intermediate, and C₄ species from three evolutionary lineages of C₄ photosynthesis. *Oecologia* 169:341–352. <https://doi.org/10.1007/s00442-011-2201-z>
- von Caemmerer S (1989) A model of photosynthetic CO₂ assimilation and carbon-isotope discrimination in leaves of certain C₃–C₄ intermediates. *Planta* 178:463–474. <https://doi.org/10.1007/bf00963816>
- von Caemmerer S (1992) Carbon isotope discrimination in C₃–C₄ intermediates. *Plant Cell Environ* 15:1063–1072. <https://doi.org/10.1111/j.1365-3040.1992.tb01656.x>
- von Caemmerer S (2000) Biochemical models of leaf photosynthesis. CSIRO Publishing, Collingwood
- von Caemmerer S (2013) Steady-state models of photosynthesis. *Plant Cell Environ* 36:1617–1630. <https://doi.org/10.1111/pce.12098>
- von Caemmerer S (2020) Rubisco carboxylase/oxygenase: from the enzyme to the globe: a gas exchange perspective. *J Plant Physiol* 252:153240. <https://doi.org/10.1016/j.jplph.2020.153240>
- von Caemmerer S (2021) Updating the steady-state model of C₄ photosynthesis. *J Exp Bot* 72:6003–6017. <https://doi.org/10.1093/jxb/erab266>
- von Caemmerer S, Farquhar GD (1981) Some relationships between the biochemistry of photosynthesis and the gas exchange of leaves. *Planta* 153:376–387. <https://doi.org/10.1007/bf00384257>
- von Cammerer S, Furbank RT (1999) Modeling of C₄ photosynthesis. In: Sage RF, Monson R (eds) C₄ plant biology. Academic Press, San Diego, pp 169–207
- von Caemmerer S, Farquhar G, Berry J (2009) Biochemical model of C₃ photosynthesis. In: Laisk A, Nedbal L, Govindjee U (eds) Photosynthesis in silico: understanding complexity from molecules to ecosystems. Springer, Dordrecht, pp 209–230
- Voznesenskaya EV, Koteleva NK, Chuong SDX, Ivanova AN, Barroca J, Craven LA, Edwards GE (2007) Physiological, anatomical and biochemical characterisation of photosynthetic types in genus *Cleome* (Cleomaceae). *Functional Plant Biol* 34:247. <https://doi.org/10.1071/fp06287>
- Wang Y, Long SP, Zhu XG (2014) Elements required for an efficient NADP-malic enzyme type C₄ photosynthesis. *Plant Physiol* 164:2231–2246. <https://doi.org/10.1104/pp.113.230284>
- Wang S, Tholen D, Zhu XG (2017) C₄ photosynthesis in C₃ rice: a theoretical analysis of biochemical and anatomical factors. *Plant Cell Environ* 40:80–94. <https://doi.org/10.1111/pce.12834>
- Wang Y, Chan KX, Long SP (2021) Towards a dynamic photosynthesis model to guide yield improvement in C₄ crops. *Plant J* 107:343–359. <https://doi.org/10.1111/tpj.15365>
- Way DA, Katul GG, Manzoni S, Vico G (2014) Increasing water use efficiency along the C₃ to C₄ evolutionary pathway: a stomatal optimization perspective. *J Exp Bot* 65:3683–3693. <https://doi.org/10.1093/jxb/eru205>
- Weis E, Ball JT, Berry JA (1987) Photosynthetic control of electron transport in leaves of *Phaseolus vulgaris*: evidence for regulation of photosystem 2 by the proton gradient. In: Biggens J (ed) Progress in photosynthesis research. Springer, Dordrecht, pp 553–556
- Westhoff P, Gowik U (2004) Evolution of C₄ phosphoenolpyruvate carboxylase. Genes and proteins: a case study with the genus *Flaveria*. *Ann Bot* 93:13–23. <https://doi.org/10.1093/aob/mch003>
- Woo K, Osmond C (1976) Glycine decarboxylation in mitochondria isolated from spinach leaves. *Aust J Plant Physiol* 3:771–785. <https://doi.org/10.1071/pp9760771>
- Woodrow IE, Berry JA (1988) Enzymatic regulation of photosynthetic CO₂ fixation in C₃ plants. *Annu Rev Plant Phys* 39:533–594. <https://doi.org/10.1146/annurev.pp.39.060188.002533>
- Yamori W, Hikosaka K, Way DA (2014) Temperature response of photosynthesis in C₃, C₄, and CAM plants: temperature acclimation and temperature adaptation. *Photosynth Res* 119:101–117. <https://doi.org/10.1007/s11120-013-9874-6>
- Yin X, Struik PC (2012) Mathematical review of the energy transduction stoichiometries of C₄ leaf photosynthesis under limiting light. *Plant Cell Environ* 35:1299–1312. <https://doi.org/10.1111/j.1365-3040.2012.02490.x>
- Yin X, Struik PC (2018) The energy budget in C₄ photosynthesis: insights from a cell-type-specific electron transport model. *New Phytol* 218:986–998. <https://doi.org/10.1111/nph.15051>
- Yin X, Struik PC (2021) Exploiting differences in the energy budget among C₄ subtypes to improve crop productivity. *New Phytol* 229:2400–2409. <https://doi.org/10.1111/nph.17011>
- Yin X, Struik PC, Romero P, Harbinson J, Evers JB, van der Putten PEL, Vos J (2009) Using combined measurements of gas exchange and chlorophyll fluorescence to estimate parameters of a biochemical C₃ photosynthesis model: a critical appraisal and a new integrated approach applied to leaves in a wheat (*Triticum aestivum*) canopy. *Plant Cell Environ* 32:448–464. <https://doi.org/10.1111/j.1365-3040.2009.01934.x>
- Yin X, Sun Z, Struik PC, van der Putten PEL, van Ieperen W, Harbinson J (2011) Using a biochemical C₄ photosynthesis model and combined gas exchange and chlorophyll fluorescence measurements to estimate bundle-sheath conductance of maize leaves differing in age and nitrogen content. *Plant Cell Environ* 34:2183–2199. <https://doi.org/10.1111/j.1365-3040.2011.02414.x>
- Zhou H, Akçay E, Helliker BR (2019) Estimating C₄ photosynthesis parameters by fitting intensive A/Ci curves. *Photosynth Res* 141:181–194. <https://doi.org/10.1007/s11120-019-00619-8>
- Zhu X-G, Wang YU, Ort DR, Long SP (2013) e-photosynthesis: a comprehensive dynamic mechanistic model of C₃ photosynthesis: from light capture to sucrose synthesis. *Plant Cell Environ* 36:1711–1727. <https://doi.org/10.1111/pce.12025>